chemosensors

MDPI

Article

Networked Low-Cost Sensor Systems for Urban Air Quality Monitoring: A Long-Term Use-Case in Bari (Italy)

Michele Penza *, Domenico Suriano , Valerio Pfister, Sebastiano Dipinto, Mario Prato and Gennaro Cassano

ENEA—Italian National Agency for New Technologies, Energy and Sustainable Economic Development, Laboratory Functional Materials and Technologies for Sustainable Applications, Brindisi Research Centre, Strada Statale 7, Appia, Km. 706, I-72100 Brindisi, Italy; domenico.suriano@enea.it (D.S.); valerio.pfister@enea.it (V.P.); dipintosebastiano@gmail.com (S.D.); mario.prato@enea.it (M.P.); gennaro.cassano@enea.it (G.C.)
* Correspondence: michele.penza@enea.it; Tel.: +39-0831-201422

Abstract

A sensor network based on 10 stationary nodes distributed in Bari (Southern Italy) has been deployed for urban air quality (AQ) monitoring. The low-cost sensor systems have been installed in specific sites (e.g., buildings, offices, schools, streets, ports, and airports) to enhance environmental awareness of the citizens and to supplement the expensive official air-monitoring stations with cost-effective sensor nodes at high spatial and temporal resolution. Continuous measurements were performed by low-cost electrochemical gas sensors (CO, NO_2, O_3), optical particle counter (PM_{10}), and NDIR infrared sensor (CO_2), including micro-sensors for temperature and relative humidity. The sensors are operated to assess the performance during a campaign (July 2015–December 2017) of several months for citizen science in sustainable smart cities. Typical values of CO_2, measured by distributed nodes, varied from 312 to 494 ppm (2016), and from 371 to 527 ppm (2017), depending on seasonal micro-climate change and site-specific conditions. The results of the AQ-monitoring long-term campaign for selected sensor nodes are presented with a relative error of 26.2% (PM_{10}), 21.7% (O_3), 25.5% (NO_2), and 79.4% (CO). These interesting results suggest a partial compliance, excluding CO, with Data Quality Objectives (DQO) by the European Air Quality Directive (2008/50/EC) for Indicative (Informative) Measurements.

Keywords: air quality sensors; gas sensors; particulate matter devices; low-cost sensor-systems; wireless sensors network; urban air quality monitoring; air quality EC directive

check for updates

Received: 2 May 2025
Revised: 18 September 2025
Accepted: 29 September 2025
Published: 28 October 2025

Citation: Penza, M.; Suriano, D.; Pfister, V.; Dipinto, S.; Prato, M.; Cassano, G. Networked Low-Cost Sensor Systems for Urban Air Quality Monitoring: A Long-Term Use-Case in Bari (Italy). *Chemosensors* **2025**, *13*, 380. https://doi.org/10.3390/chemosensors13110380

1. Introduction

1.1. Background and Motivation

Urban air quality is a major issue for public health, especially in megacities. The UN Environment Program Report 2016 [1] reported that many worldwide cities do not meet the requirements for cleaner air. Air pollution is still the principal environmental cause of premature deaths in the European Union, as reported by the European Environment Agency (EEA) Report 2017 [2] and Report 2024 [3]. In fact, air pollution is causing more than 400,000 premature deaths each year. Furthermore, millions of Europeans suffer from respiratory and cardiovascular diseases caused by air pollution: NO_2, O_3, SO_2, and particulate matter (PM) are identified as key species affecting quality of life and mortality rates, as reported by the World Health Organization (WHO) Report 2006 [4]. Also, CO, NO_2, and fine particulate matter are known to affect respiratory and cardiovascular diseases. The costs of air pollution in the European Union are well over €20 billion a year. To mitigate these negative effects of air pollution on human health, environment, and eco-systems, the European Commission adopted the *Ambient Air Quality Directive* (2008/50/EC) [5] and the successive Directive EU 2024/2881 of the European Parliament and of the Council of 23 October 2024 on *Ambient Air Quality and Cleaner Air for Europe* [6] that fixed stringent thresholds for each pollutant.

Currently, low-cost sensors (LCS) are gaining importance in monitoring air quality at high spatial and temporal resolutions [7]. In fact, the World Meteorological Organization (WMO) supported LCS for the measurement of atmospheric composition as a future application for environmental monitoring [8]. Also, the US Environmental Protection Agency (EPA) deliberated standards and performance targets for air-quality sensors [9]. A unified terminology for LCS has been proposed to label different levels of sensor systems and sensor networks [10]. Some limitations in air sensors' performance still exist, such as sensitivity, selectivity, stability, limit of detection, drift, repeatability, and so on. Current trends to overcome these low operations explore functional materials, nanomaterials, and nanotechnologies [11], and advanced and hybrid transducers [12].

Furthermore, climate change monitoring is crucial to implement abatement strategies of greenhouse gases and CO_2 emissions for a low-carbon footprint in sustainable cities. In recent years, low-cost sensor systems [13–15] and sensor networks [16–19] for air-quality monitoring have been demonstrated in the real world for performance assessment, environmental awareness, personal exposure, compliance, legislative purposes, and decision support. In this study, we have performed a long-term use case using air sensors deployed in Bari city, Italy.

1.2. Case-Studies of City Sensor Networks for Air-Quality Monitoring

In recent years, an increasing number of case studies related to the use of portable sensors and sensor networks for urban air-quality monitoring have been demonstrated. The MESSAGE (Mobile Environment Sensor System Across GRID Environments) project, funded by the UK during 2006–2009, included small cost sensors (CO, NO_2, and NO) to increase the amount of data available for modelling pollution emission and dispersion [20,21]. The University of Cambridge, Newcastle University, and Imperial College London were key research leaders. Furthermore, the SNAQ-Heathrow (Sensor Network Air Quality-Heathrow) project has deployed a high-density air quality sensor network in and around London Heathrow airport. This used state-of-the-art low-cost sensors for selected gases and for particulates, providing an unprecedented dataset. The project was funded by NERC from January 2011 to December 2014 [22]. The objective was the creation of a calibrated, high spatial and temporal resolution dataset including NO, NO_2, CO, CO_2, SO_2, O_3, VOCs, and size-speciated PM for further scientific and policy studies. Furthermore, the OPEN-SENSE project analyzed the largest spatially resolved UFP (Ultra Fine Particle) dataset containing over 50 million measurements. The project [23] collected the measurements throughout more than two years using mobile sensor nodes installed on top of public transport vehicles in the cities of Zurich and Basel, Switzerland. Based on these data, land-use regression models have been developed to create pollution maps with a high spatial resolution of 100 mt $\times$ 100 mt. Fishbain et al. [24] reviewed the mathematical tools available for assessment of the performance of air quality micro-sensing units using data collected in eight European cities of the FP7 project CITI-SENSE. Recently, the Copenhagen Wheel developed an electric bike technology living inside a red hub connected to a smartphone. There are no buttons, wires, or external batteries. The Wheel's custom sensors, computers, battery, and motor do the rest for measuring air quality in Copenhagen [25]. L. Sun et al. [26] developed a sensor network used to monitor air quality during a marathon in 2015 in Hong Kong. In Beijing, China, a city network based on 2500 sensor nodes for

$PM_{2.5}$ detection is operated by the local environmental authority for decision support. J. Zhang et al. [27] developed a portable farmland information collection system with multiple sensors for air-quality monitoring in China. S. Choi et al. [28] developed a micro-sensor node for air-pollutant monitoring in Korea. T.F. Villa et al. [29] developed an Unmanned Aerial Vehicle (UAV)-based system for air pollution measurements in Australia. J. Kim et al. [30] developed a sensor network based on 50 nodes distributed at Berkeley (California) for air-quality monitoring (CO, NO, NO_2, O_3, CO_2, and PM_{10}). The CLAIRITY project [31] developed an air quality network near the Massachusetts Institute of Technology (MIT) in Boston, USA.

Further case studies of low-cost sensor networks deployed for urban air-quality monitoring have been extensively investigated worldwide. In Europe, R.L. Jones' team [32] studied a wireless sensor network (WSN) for source attribution of air pollution and operated in Cambridge city, UK; V. van Zoest et al. [33] investigated a field-calibrated NO_2-based WSN in Eindhoven city, Holland. Kaminska et al. [34] reported a study conducted in Wrocław (Poland) in October 2021, combining data on eBC (equivalent of black carbon) concentration (measured by microaethalometer), air quality (from the national environmental monitoring system), and traffic (from the municipal traffic management system). The aim of this research was to estimate, by an indirect approach, the relation between eBC concentration and other air pollutants in order to create more sustainable cities. Also, in Israel, Yuval et al. [35] demonstrated an optical particle counter (OPC) network for assessment of emission impact as operated in Elad city.

In the Americas, D.H. Hagan et al. [36] studied the calibration and assessment of the electrochemical air quality sensors by co-location with regulatory-grade instruments in Hawaii, USA. S.N. Feinberg et al. [37] examined the spatiotemporal variability of urban particulate matter using data from a network of low-cost air pollution sensors operated in the Memphis area, USA. Kimbrough et al. [38] proposed a Local-Scale Air Quality Study integrating low-cost sensors and reference-grade monitoring in a complex metropolitan area in Kansas City, USA. G. Miskell et al. [39] demonstrated reliable data from low-cost ozone sensors in a hierarchical network as deployed in the Los Angeles area, USA. A. Collier-Oxandale et al. [40] evaluated the field and laboratory performance of 28 gas-phase air quality sensors by the AQ-SPEC (Air Quality Sensor Performance Evaluation Centre) programme as deployed in the Los Angeles area, USA. Also, in Brazil, D. da Silva Sousa et al. [41] developed an automated, self-powered, and integrated analytical platform for online and in situ air-quality monitoring as tested in two Brazilian cities from the San-Paulo region.

In Asia, Wei et al. [42] studied the impact of temperature and humidity on electrochemical sensors' (CO, NO, NO_2, and O_3) response in ambient air-quality monitoring in Hong Kong, China. Wang et al. [43] demonstrated the application of machine learning for the in-field correction of a $PM_{2.5}$ low-cost sensor network in Taipei, Taiwan. Cao et al. [44] deployed a distributed air-sensor network to investigate the spatiotemporal patterns of $PM_{2.5}$ concentrations in Dezhou city, China.

1.3. Ambient Air Quality EU Directive

The Ambient Air Quality EU Directive (2008/50/EC) defines two different regimes of measurements: (a) *Fixed Measurements* and (b) *Indicative Measurements* (*Informative Measurements*). The former mean measurements were taken at fixed sites to determine the air pollution levels in accordance with the relevant Data Quality Objectives (DQO), provided by reference instrumentation only. The fixed measurements are mandatory in zones and agglomerations where the upper assessment thresholds are exceeded. The latter mean measurements meet DQOs that are less strict than those required for fixed measurements.

The DQOs of the Indicative Measurements can be addressed by air quality low-cost sensors. The uncertainty for fixed measurements is as follows: 15% ($NO_x/NO_2/NO$, CO, SO_2); 25% (Benzene); 15% (O_3); and 30% ($PM_{10}/PM_{2.5}$). On the contrary, the uncertainty for Indicative Measurements is as follows: 25% ($NO_x/NO_2/NO$, CO, SO_2); 30% (Benzene); 30% (O_3); and 50% ($PM_{10}/PM_{2.5}$). The EU Directive does not include CO_2 as a compound of interest, but CO_2 is an indicator for traffic and greenhouse emissions. A rough estimation of the uncertainty should range from 5 to 10%, as provided by the actual limits of the CO_2 sensor performance for real applications.

Further details on uncertainties that are useful for *Indicative Measurements* to be achieved by low-cost sensors for air-quality monitoring are reported in Appendix B, as recently updated by *Directive of the European Parliament and of the Council on Ambient Air Quality and Cleaner Air for Europe* [6], dated 14 October 2024 (PE-CONS 88/24).

1.4. Aim of Work

Bari is a metropolitan city in Southern Italy of about five hundred thousand people (ninth position in Italy and third position in Southern Italy) with an economy based on commerce, manufacturing, and a knowledge economy. The transportation system is globally inter-operative, with a local surface network, port, and international airport. Bari is the headquarters of two Public Universities (Sciences, Engineering, Literature, Social, Law, Economy, and Medicine) with about sixty thousand students. The city is a member of the European Covenant of Mayors for Climate and Energy. This urban eco-system is a perfect real scenario for a long-term campaign for the air quality sensor network.

The present study on air quality sensor networks for urban monitoring is strongly linked to previous works from the author team related to the application of low-cost sensors in urban areas such as city centres, industrial zones, and airports [45–47].

In this study, the performance of the sensor network for urban air-quality monitoring has been assessed in the city of Bari by 30-month long-term measurements. The sensor data is compared to the reference environmental public data to evaluate the accuracy and data quality objectives of the European Air Quality Directive (2008/50/EC) for Indicative Measurements.

2. Materials and Methods

2.1. Sensor Nodes

The sensor nodes, AIRBOX, shown in Figure 1, were designed to be small in size (23 cm width × 30 cm height × 10 cm depth), thermoplastic weatherproof (IP 65/66), able to operate on their own, and connected to power. The compact size of the sensor node was useful to facilitate deployment and reduce the installation footprint. Each sensor node includes a suite of 9 low-cost sensors: 4 electrochemical gas sensors: NO_2, O_3, CO, and SO_2 (not considered in this study); 1 Near Dispersive Infra-Red (NDIR) sensor: CO_2; 1 Photo-Ionization Detector (PID): total Volatile Organic Compounds (tVOCs); 1 Particulate Matter sensor: PM_{10}; 1 temperature (T) sensor; and 1 relative humidity (RH) sensor. The components are listed in Table 1. These sensors were selected due to their low-power consumption (<10 mW for the electrochemical sensor, and <60 mW for the NDIR sensor) and their low-voltage operation (3.3–5.0 Vcc), including good sensitivity and low limit of detection at the ppb level of environmental interest.

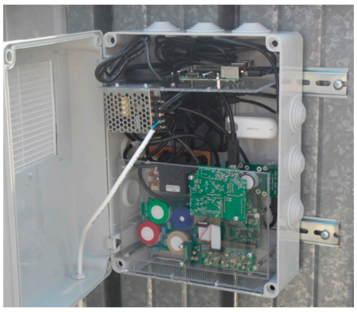

Figure 1. Sensor node AIRBOX, developed by ENEA, for urban air pollution monitoring.

Table 1. List of gas/particulate matter and environmental sensors installed in each AIRBOX sensor node for urban air-quality monitoring.

Pollutant	Sensor Type	Manufacturer	Characteristics	Principle of Operation
CO	CO-B4	Alphasense, UK	0–20 ppm	Electrochemical
NO_2	NO_2-B4	Alphasense, UK	0–2 ppm	Electrochemical
O_3	O_3-B4	Alphasense, UK	0–2 ppm	Electrochemical
SO_2	SO_2-B4	Alphasense, UK	0–2 ppm	Electrochemical
CO_2	CO_2-IRC-A1	Alphasense, UK	0–5000 ppm	NDIR
VOCs	VOCs-PID-A1	Alphasense, UK	0–100 ppm	Photo-ionization
PM_{10}	PPD20V	Shinyei, Japan	0–100 $\mu g/m^3$	Light scattering
Temperature	TC1047A	Microchip	-40 ± 125 °C	Thermo-converter
Relative Humidity	HIH5031	Honeywell	0–90%	Capacitive

The sensor node incorporates a Raspberry Pi-based computer (Model B+) with 4 USB ports, 1 Ethernet port, and 512 Mb RAM, using the open-source operating system Linux for data acquisition management by an SD card (2 Gb) for on-board data logging.

The remote node uses a GPRS modem (Key HSPA Huawei E303) with a SIM card, operated by a public provider, to transmit data to a central server (Dell, Model PowerEdge R320, 6 core-Intel Xeon, 16 Gb RAM, 6 discs by 500 Gb in raid5 configured) with a pack sampling rate to be configured properly.

Additionally, a Wi-Fi key (Edimax USB 2.0, 802.11, 2.4 GHz, 150 Mbit/s) is installed for city operation covered by a digital network. Finally, a Global Positioning System (GPS) receiver (Garmin, Model GPS 18× USB) was used for convenient deployment, mainly for mobile sensing purposes.

2.2. Sensor Network

A sensor network based on 10 AIRBOX stationary nodes has been deployed for urban air-quality monitoring in the city of Bari (Southern Italy).

The sensor nodes have been installed in the external areas (roofs, windows, terraces, and balconies) of the specific sites (buildings, offices, schools, streets, ports, and airports), selecting the available operating site as close as possible to a reference air-quality monitoring station managed by ARPA-Puglia to validate sensor data.

All nodes, shown in Figure 2, are deployed in an urban area of 24 km^2: 6 nodes are located in the city area with a mean distance of less than 1 km from the Adriatic sea; and 4 nodes are located in the tangential road area at high vehicular traffic, including 3 nodes operated in the industrial zone.

(**a**)

(**b**)

Air-Quality Monitoring Stations in Bari	**Picture of Air Quality Stations**	**Description of Station**
ARPA Puglia-Viale Kennedy		• Air Monitors: NO_2, O_3, PM_{10}, $PM_{2.5}$ • Station type: Urban (Background) • Analyzer type: Chemiluminescence (NO-NO_2-NO_x) Photometry UV (O_3) Light Scattering (PM)
ARPA Puglia-Via Caldarola		• Air Monitors: NO_2, C_6H_6, CO, $PM_{2.5}$ • Station type: Urban (Traffic) • Analyzer type: Chemiluminescence (NO-NO_2-NO_x) Photo-Ionization (BTX) Spectroscopy IR (CO) Light Scattering (PM)
ARPA Puglia-Modugno EN4		• Air Monitors: NO_2, PM_{10}, CO • Station type: Sub-Urban • Analyzer type: Chemiluminescence (NO-NO_2-NO_x) Spectroscopy IR (CO) Light Scattering (PM)

Figure 2. *Cont.*

ARPA Puglia-Modugno EN2		• Air Monitors: NO_2, O_3, CO, PM_{10}, $PM_{2.5}$ • Station type: Sub-Urban • Analyzer type: Chemiluminescence (NO-NO_2-NO_x) Photometry UV (O_3) Spectroscopy IR (CO) Light Scattering (PM)
ARPA Puglia-Carbonara		• Air Monitors: NO_2, PM_{10} • Station type: Sub-Urban (Background) • Analyzer type: Chemiluminescence (NO-NO_2-NO_x) Light Scattering (PM)
ARPA Puglia-Via Cavour		• Air Monitors: NO_2, C_6H_6, CO, PM_{10}, $PM_{2.5}$ • Station type: Urban (Traffic) • Analyzer type: Chemiluminescence (NO-NO_2-NO_x) Spectroscopy IR (CO) Photo-Ionization (BTX) Light Scattering (PM)
ARPA Puglia-CUS Bari		• Air Monitors: NO_2, O_3, PM_{10} • Station type: Sub-Urban (Traffic) • Analyzer type: Chemiluminescence (NO-NO_2-NO_x) Photometry UV (O_3) Light Scattering (PM)

Figure 2. (**a**) Sensor nodes AIRBOX deployed in Bari city for air-quality monitoring. (**b**) Reference monitoring stations deployed in Bari city for air-quality monitoring.

Table 2 summarizes the location of sensor nodes to be referenced with the closest air quality station.

Table 2. List of the sensor nodes deployed in Bari city and managed by ENEA in the period of the campaign from 1 July 2015 to 31 December 2017. The air-quality monitoring stations of the local environmental agency (ARPA-Puglia) closest to the deployed sensor nodes are indicated with the related Universal Transverse Mercator (UTM) coordinate system.

Node ID	Node Location	Sensor Node Coordinates		Closest ARPA-Puglia Air Quality Monitoring Station	AQM Station UTM33 Coordinates		Distance Sensor Node and AQM Station (km)
		Long. East (UTM33)	Lat. North (UTM33)		Long. East	Lat. North	
Node 1	ENELVia Capruzzi	16.87370 (657305)	41.11720 (4553459)	ARPAViale Kennedy	656105	4551478	2.1

Table 2. *Cont.*

Node ID	Node Location	Sensor Node Coordinates		Closest ARPA-Puglia Air Quality Monitoring Station	AQM Station UTM33 Coordinates		Distance Sensor Node and AQM Station (km)
		Long. East (UTM33)	Lat. North (UTM33)		Long. East	Lat. North	
Node 2	ENEAViale Japigia	16.89963 (659494)	41.11259 (4552995)	ARPAVia Caldarola	658520	4553079	1.4
Node 3	PERONIVia Bitritto	16.84361 (654830)	41.09558 (4551005)	ARPAModugno EN4	650120	4553064	6.1
Node 4	AMTABVia Jacobini	16.80469 (651516)	41.11529 (4553125)	ARPAModugno EN4	650120	4553064	6.0
Node 6	AIRPORT WojtylaViale Ferrari	16.77646 (649090)	41.13979 (4555796)	ARPAModugno EN2	648305	4555516	8.8
Node 7	MOBILEon a public bus	-	-	-	-	-	
Node 8	POLITECNICOVia Amendola	16.88335 (658130)	41.11126 (4552817)	ARPAVia Caldarola	658520	4553079	0.8
Node 9	COFELYStrada Vassallo	16.87113 (657148)	41.09260 (4550724)	ARPACarbonara	654377	4598816	2.2
Node 10	UFFICI COMUNALIPiazza Ferrarese	16.87206 (657145)	41.12676 (4554518)	ARPAVia Cavour	657197	4554020	0.8
Node 11	FAIRLungomare Starita	16.839167 (654361)	41.136389 (4555528)	ARPACUS Bari	654877	4555353	0.7
Node 12	PORTMolo San Vito	16.5100 (626852)	41.0748 (4548159)	ARPACUS Bari	654877	4555353	0.7

2.3. Virtual Private Network and Server

A Virtual Private Network (VPN) has been implemented to communicate by secure digital certificate with each remote node (*nasuspi-x*) using TCP/IP protocol (IPv4). The VPN scheme is shown in Figure 3. The software used for data acquisition management is open-source Python (version 3.11). The sampling rate for each node is 10 s. The data are locally stored in each node and transmitted every 60 min towards the central server (Dell, Model PowerEdge R320, 6 core-Intel Xeon, 16 Gb RAM, 6 discs by 500 Gb in raid5 configured). Data from each remote node has been uploaded and stored on the central server, hosted by ENEA, and displayed on a private web page accessed with signed credentials. The web page displays data in a tabular format to support the direct download. The data acquired by each virtual node (*nasuspi-x*) is useful for automatic post-processing in the dedicated webGIS page.

2.4. Global Information System

Figure 4 shows the screenshot of the web Global Information System to manage the visualization of the sensor network in the framework of the national project RES-NOVAE, including measurement setup for individual nodes, selection of node to be visualized, mean at hourly, daily, monthly, and yearly steps for individual AQI, and related absolute value of gas concentration of any measured pollutant in restricted areas. Moreover, it is possible to select data, both in tabular and graphic form, related to the period of the measurements of interest for analysis and post-processing.

ENEA Sensors Lab OpenVPN Status Monitor

Enea NasusPI - Connection up, pingable. 11 clients, 200477075 bytes in, 102772056 bytes out [172.17.0.1 tun]

Username / Hostname	VPN IP Address	Remote IP Address	Port	Location	Recv	Sent	Connected Since	Last Ping	Time Online
nasuspi-10	172.17.0.11	5.170.131.238	58515		1806327	873776	29/11/2015 10:11:44	30/11/2015 10:25:44	1 day, 0:20:03
nasuspi-1	172.17.0.2	5.170.172.198	30993		8496665	4153071	25/11/2015 15:32:25	30/11/2015 10:30:06	4 days, 18:59:22
nasuspi-3	172.17.0.4	5.170.40.252	9232		8283583	4053989	25/11/2015 15:57:13	30/11/2015 10:16:37	4 days, 18:34:34
airbox-one	172.17.0.20	192.168.172.238	53361	RFC1918	6032885	6382542	19/11/2015 13:53:04	19/11/2015 13:53:04	10 days, 20:38:43
nasuspi-8	172.17.0.9	5.170.174.197	11954		8290815	4083927	25/11/2015 15:52:06	30/11/2015 10:27:18	4 days, 18:39:41
nasuspi-7	172.17.0.8	62.19.59.138	36495		368480	172026	30/11/2015 06:12:21	30/11/2015 10:22:35	4:19:26
nasuspi-6	172.17.0.7	5.170.31.11	39923		8806847	4107541	25/11/2015 15:31:45	30/11/2015 10:19:11	4 days, 19:00:02
nasuspi-9	172.17.0.10	5.170.103.72	30669		5371409	2566251	27/11/2015 10:42:06	30/11/2015 10:20:57	2 days, 23:49:41
nasuspi-2	172.17.0.3	5.170.197.62	4448		8276782	4061880	25/11/2015 15:43:00	30/11/2015 10:30:10	4 days, 18:48:47
nasuspi-12	172.17.0.13	192.168.173.82	33491	RFC1918	558516	372320	30/11/2015 09:56:46	30/11/2015 10:31:47	0:35:01
nasuspi-4	172.17.0.5	5.170.226.56	28348		8362880	4068711	25/11/2015 15:30:36	30/11/2015 10:20:09	4 days, 19:01:11

Figure 3. Screenshot of the Virtual Private Network by ENEA for air-quality monitoring.

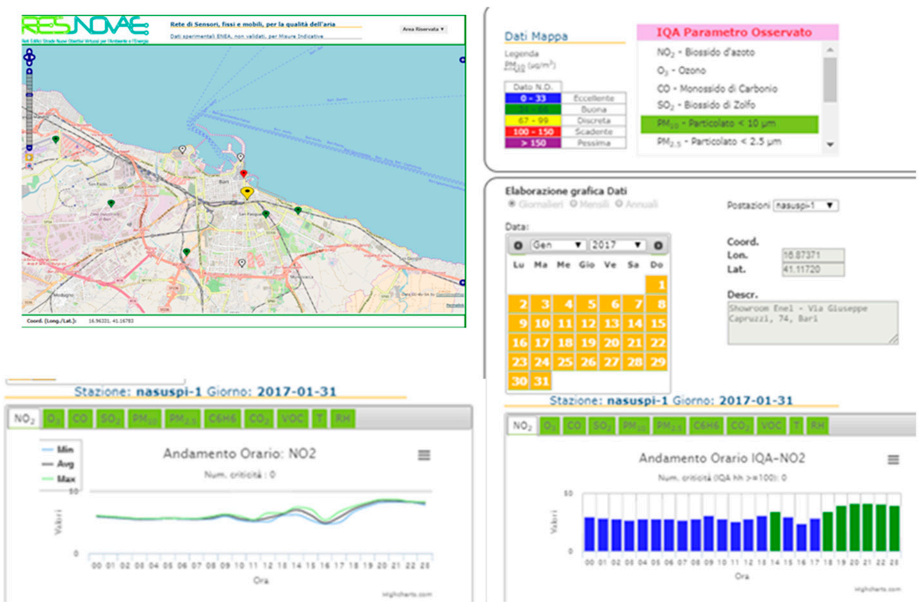

Figure 4. Screenshot of WebGIS to manage sensor network in the RES-NOVAE project with section of measurement visualization setup, ranking, and colours for individual AQI, hourly mean for selected AQI, and hourly mean for gas concentration in the restricted area. The blue bar means very clean air; while the green bar means clean air. This standard is defined in ref. [46].

Finally, an APP RES-NOVAE in the Android environment has been developed to visualize the AQI and gas concentration of a given specific node upon daily format.

2.5. Sensor Calibration

The air quality sensors used in the Bari campaign consisted of commercial low-cost electrochemical sensors for gas (NO_2, O_3, and CO) detection and a commercial cost-effective optical particle counter (OPC) for particulate matter (PM_{10}) detection, including miniaturized sensors for meteorology parameters (T and RH). Usually, these chemical sensors (gases and PM) arrive uncalibrated from the manufacturer, and thus, it is necessary to calibrate using a dedicated reference analyzer. Laboratory evaluation and in-field calibration are important to convert the output sensor signal (V) into gas concentration (ppb) and into PM concentration (μg/m^3). The lab calibration is a preliminary test before a more accurate in-field calibration to minimize the cross-contamination effects and environmental interferent (T and RH) compensation. Therefore, before the Bari campaign (October 2014), ENEA calibrated the prototypes by co-located measurements with reference analyzers in an official air-quality monitoring station at JRC, located in Ispra, Italy (45°48.881′ N, 8°38.165′ E). The in-field calibration by the co-location of sensors and reference equipment took place in Ispra from 28 January to 8 June 2014 for NO_2, O_3, CO, SO_2, and PM_{10} in order to assess the mean error of the sensors compared to the reference instrument. During this measurement period, the NO_2 concentrations varied from 5 to 40 ppb with a mean error ranging from 3 to 15 ppb, depending on environmental conditions and measured concentration range. The O_3 concentrations varied from 10 to 50 ppb with a mean error ranging from 5 to 20 ppb, depending on environmental conditions and measured concentration range. The CO concentrations varied from 200 to 600 ppb, with a mean error ranging from 90 to 170 ppb, depending on the environmental conditions and measured concentration range. The SO_2 concentrations were very low in the rural area at Ispra, and no estimation of the concentration mean error was applicable. The PM_{10} concentrations varied from 5 to 68 μg/m^3 with a mean error ranging from 3 to 10 μg/m^3, depending on environmental conditions and the measured concentration range.

The in-field calibration of the sensors, already calibrated in other similar sites at Ispra, has been performed in Bari by reference instrumentation of the closest air-quality monitoring station. The calibration curves have been adapted for the on-site campaign at Bari. The air sensors are sensitive to temperature and humidity changes, as expected. A weak, not a strong, reaction of the deployed air sensors with ambient conditions has been measured in the Bari campaign; therefore, we do not exclude sensor data that are affected under very humid conditions (>75%), as reported by Mueller et al. [48].

Finally, the field calibration of the used air sensors has been adapted at the Bari sites by an initial period of training and successive optimization depending on the specific location where the air-sensor box was deployed for experimentation.

For electrochemical gas sensors, the *concentration C* (*ppb*) was calculated as follows:

$$C = \mathrm{S}\,[(V_w - \mathrm{V}_{w0}) - (V_a - \mathrm{V}_{\mathrm{a}0})] \tag{1}$$

where S is sensor sensitivity (ppb/V or ppm/V); V_w is the working electrode voltage (V); V_a is the auxiliary electrode voltage (V); V_{w0} is the zero-air working electrode voltage (V); and $V_{\mathrm{a}0}$ is the zero-air auxiliary electrode voltage (V). The auxiliary electrode voltages affect the sensitivity of the electrochemical gas sensors ranging from 10 to 100 nA/ppm, depending on gas concentration under test and environmental ambient conditions.

For particulate matter sensors, the *concentration c* (μg/m^3) was calculated as follows:

$$c = \mathrm{A}_0 + \mathrm{S} \times \mathrm{V} \tag{2}$$

S is the sensor sensitivity [(μg/m^3)/V]; A_0 is a bias constant (μg/m^3); V is the sensor output voltage (V).

2.6. Methodology

The sensors have been deployed in Bari city at selected sites for a long-term campaign of urban air-quality monitoring. The criteria for selection of the demonstration sites are as follows: (*i*) pragmatic availability to host a sensor node on the roof of the offices, buildings, schools, port, airport, and city centre by project partners; (*ii*) power availability; (*iii*) coverage of the urban area; and (*iv*) closeness of the sensor-site to an air quality monitoring station (AQMS) by ARPA-Puglia in the Bari city. The map of the distributed sensor nodes and the related network of the reference AQMS is reported in Figure 5. The campaign started on 1 July 2015 and stopped on 31 December 2017. The huge database is composed of about 5 Gb of big data. The data of the sensor network are managed by means of ENEA VPN, WebGIS, and a server, while the public official environmental data were periodically downloaded from the official site of ARPA-Puglia [49]. The final aim of the campaign was the validation of the sensor data compared to the reference data for performance assessment.

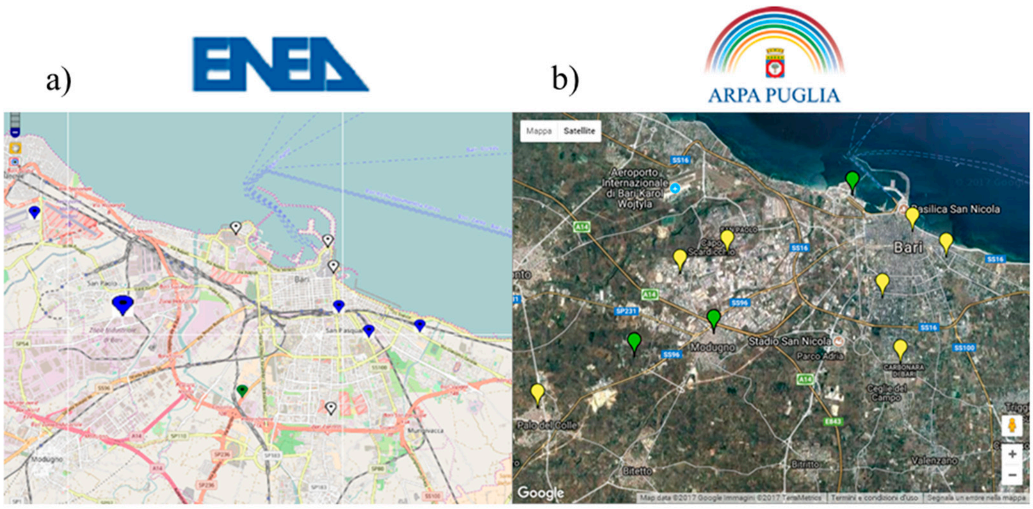

Figure 5. Map of (**a**) 10 stationary sensor nodes, managed by ENEA, deployed at Bari, and (**b**) 10 public Air-Quality Monitoring Stations (AQMS), managed by ARPA-Puglia, at Bari. The list of AQMS is reported in Table 2.

3. Results

3.1. Stationary Sensor Network Versus Reference Methods

Figures 6–11 show the time series of the daily mean of a given sensor node (Node 1: ENEL) compared to the closest air quality monitoring station (AQMS) in Bari city for the selected months of August 2015, December 2015, March 2016, October 2016, April 2017, and December 2017. The previously mentioned six months cover all four seasons during the experimental campaign (1 July 2015–31 December 2017) in order to study the different climate conditions affecting urban air pollution. The monitored air pollutants, including PM_{10}, NO_2, O_3, and CO, have been selected due to official public reference data available from the Environmental Protection Agency. The comparison of the performance between the sensor node and reference analyzer is expressed by a simple figure of merit, the Mean Absolute Error (MAE). It varies for PM_{10} from 4.88 μg/m^3 (August 2015) to 14.67 μg/m^3 (December 2017); for NO_2 from 9.22 ppb (October 2016) to 15.18 ppb (April 2017); for O_3 from 4.81 ppb (December 2016) to 16.62 ppb (August 2015); and, finally, for CO from 0.12 ppm (April 2017) to 0.40 ppm (October 2016). These results indicate a good performance of the PM_{10}, O_3, and CO sensors of Node 1, while a worse performance has been recorded for the NO_2 sensor. Additionally, the official rate of the released air-pollutant concentration is the daily mean, so no real variability during the whole day can be appreciated by this time resolution. Moreover, the CO and NO_2 concentration during the month under investigation, as measured by the Node 1 (ENEL) in Figures 6–11, is almost constant due to the location of the sensor-node (Node 1) near an urban street at high traffic, as referenced by the closest air-quality monitoring station (ARPA-Viale Kennedy). Furthermore, the PM_{10} peak, recorded on 23 March 2016 (see

Figure 8) as 78 μg/m³ measured by the sensor and 81 μg/m³ measured by the analyzer, is attributed to Saharan dust in Bari city, as certified by ARPA-Puglia.

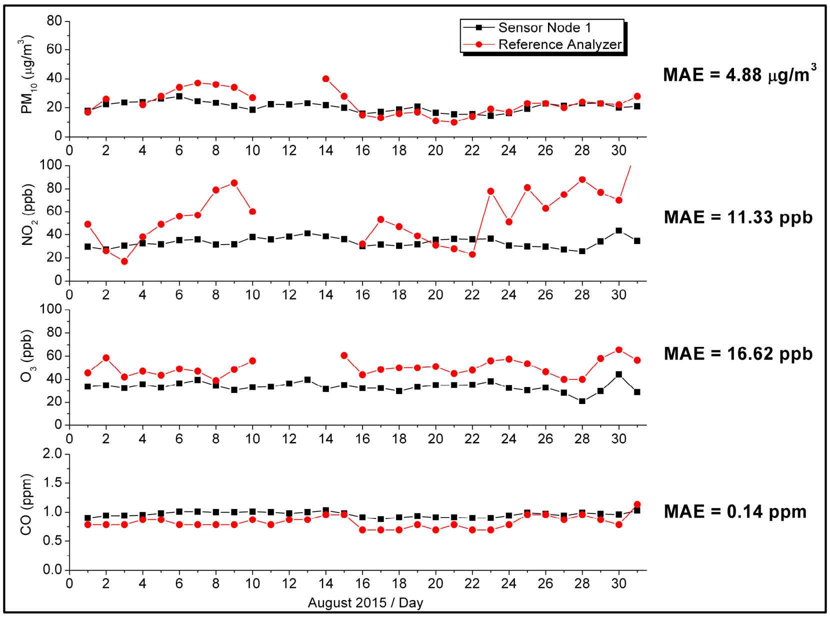

Figure 6. Comparison of the daily mean in August 2015 of a sensor (Node 1) and related reference analyzer (Viale Kennedy: PM_{10}, NO_2, and O_3, and Via Cavour: CO) deployed in the Bari city. The Mean Absolute Error (MAE) values are reported for each pollutant. Some analyzer data are missed.

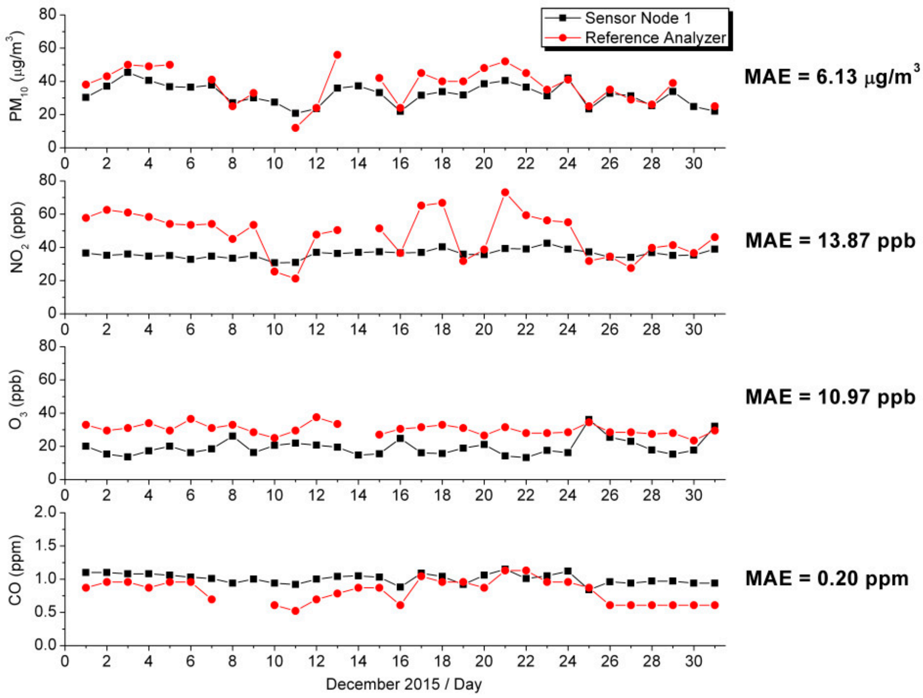

Figure 7. Comparison of the daily mean in December 2015 of a sensor (Node 1) and related reference analyzer (Viale Kennedy: PM_{10}, NO_2, and O_3, and Via Cavour: CO) deployed in the Bari city. The Mean Absolute Error (MAE) values are reported for each pollutant. Some analyzer data are missed.

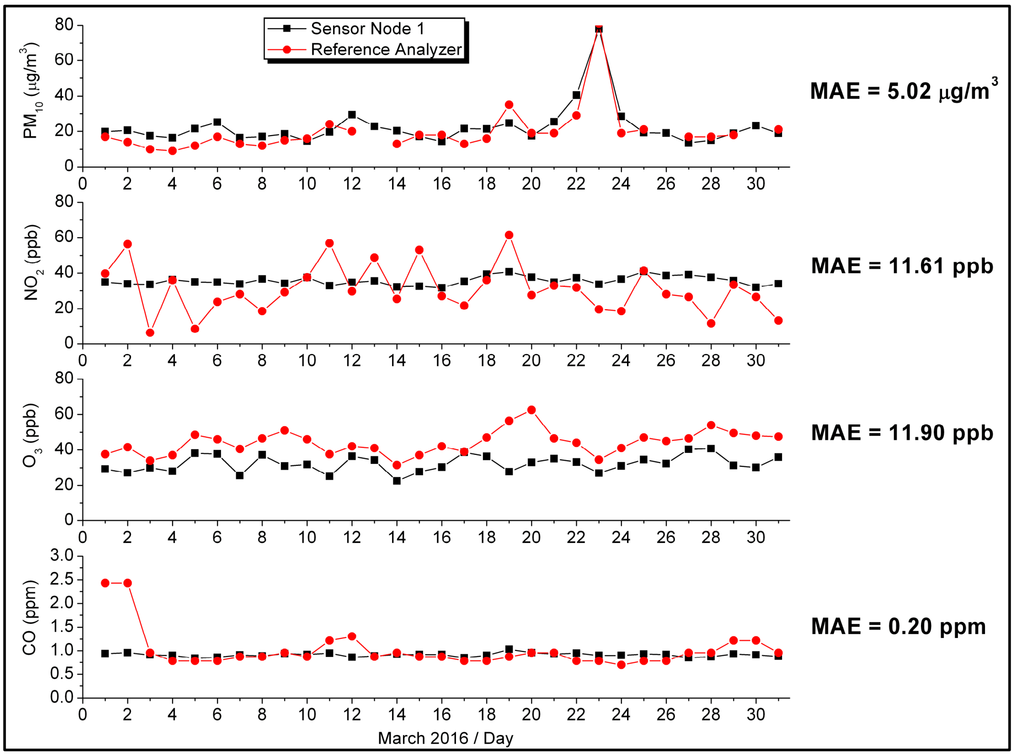

Figure 8. Comparison of the daily mean in March 2016 of a sensor (Node 1) and related reference analyzer (Viale Kennedy: PM_{10}, NO_2, and O_3, and Via Cavour: CO) deployed in the Bari city. The Mean Absolute Error (MAE) values are reported for each pollutant. Some analyzer data are missed.

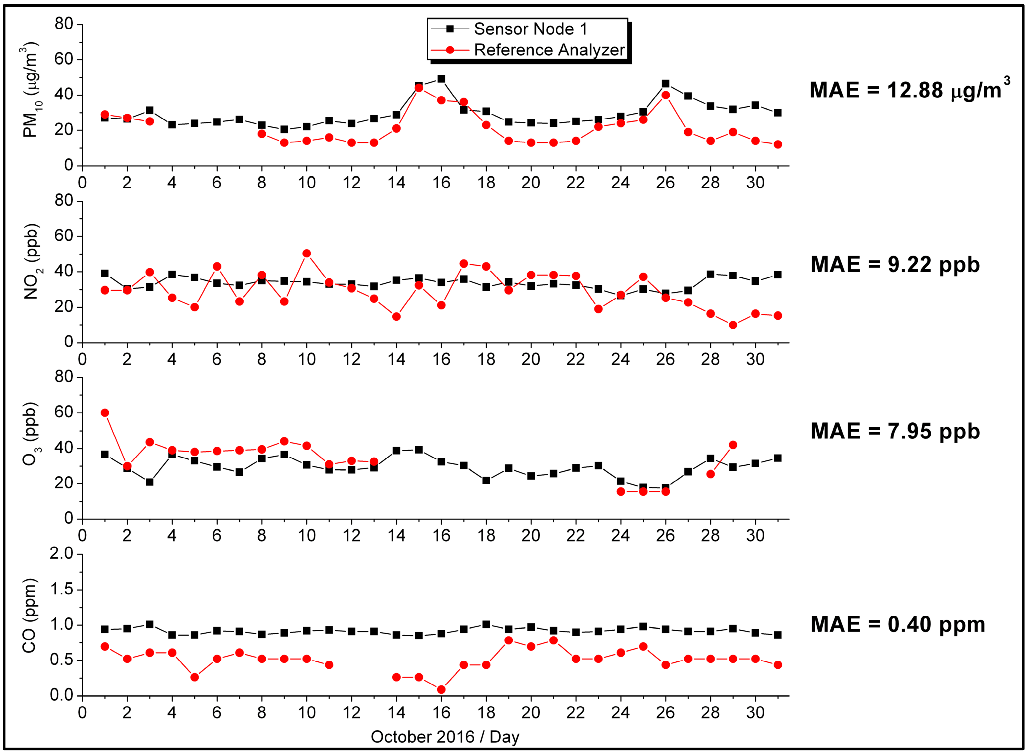

Figure 9. Comparison of the daily mean in October 2016 of a sensor (Node 1) and related reference analyzer (Viale Kennedy: PM_{10}, NO_2, and O_3, and Via Cavour: CO) deployed in the Bari city. The Mean Absolute Error (MAE) values are reported for each pollutant. Some analyzer data are missed.

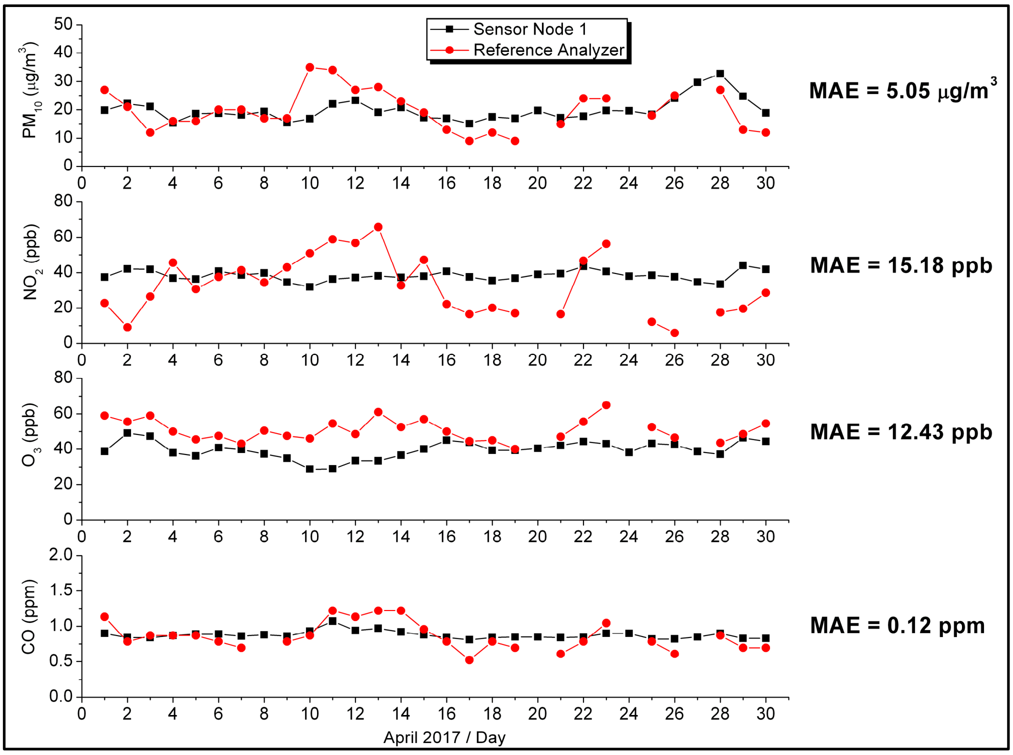

Figure 10. Comparison of the daily mean in April 2017 of a sensor (Node 1) and related reference analyzer (Viale Kennedy: PM_{10}, NO_2, and O_3, and Via Cavour: CO) deployed in the Bari city. The Mean Absolute Error (MAE) values are reported for each pollutant. Some analyzer data are missed.

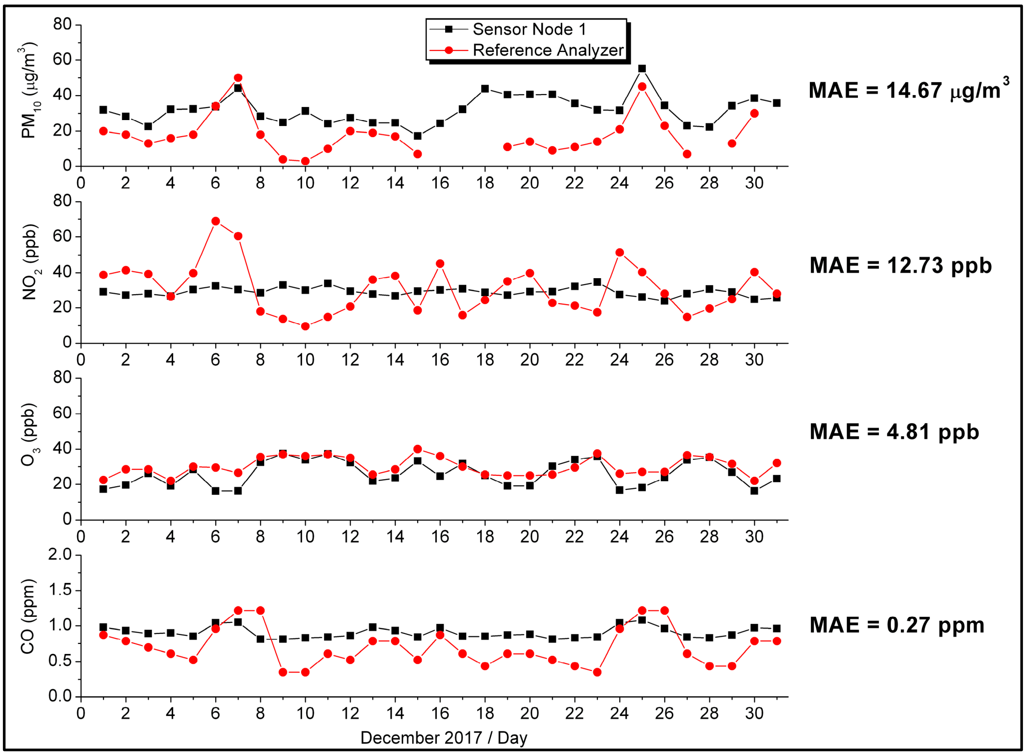

Figure 11. Comparison of the daily mean in December 2017 of a sensor (Node 1) and related reference analyzer (Viale Kennedy: PM_{10}, NO_2, and O_3, and Via Cavour: CO) deployed in Bari city. The Mean Absolute Error (MAE) values are reported for each pollutant. Some analyzer data are missed.

3.2. Sensor Network Performance

Figure 12 shows the 2016 and 2017 yearly means of the PM_{10}, NO_2, O_3, and CO of the sensor network (eight nodes) compared to the selected air quality monitoring station (AQMS) in Bari city. The ARPA-Viale Kennedy AQMS is of the urban background in the city centre and is equipped with PM_{10}, NO_2, and O_3 analyzers, but without a CO analyzer, referenced alternately by the ARPA-Via Cavour AQMS located in the city centre and categorized as an urban traffic station. The mean of the selected reference analyzers has been chosen in June 2016 and June 2017 as annual mid-term.

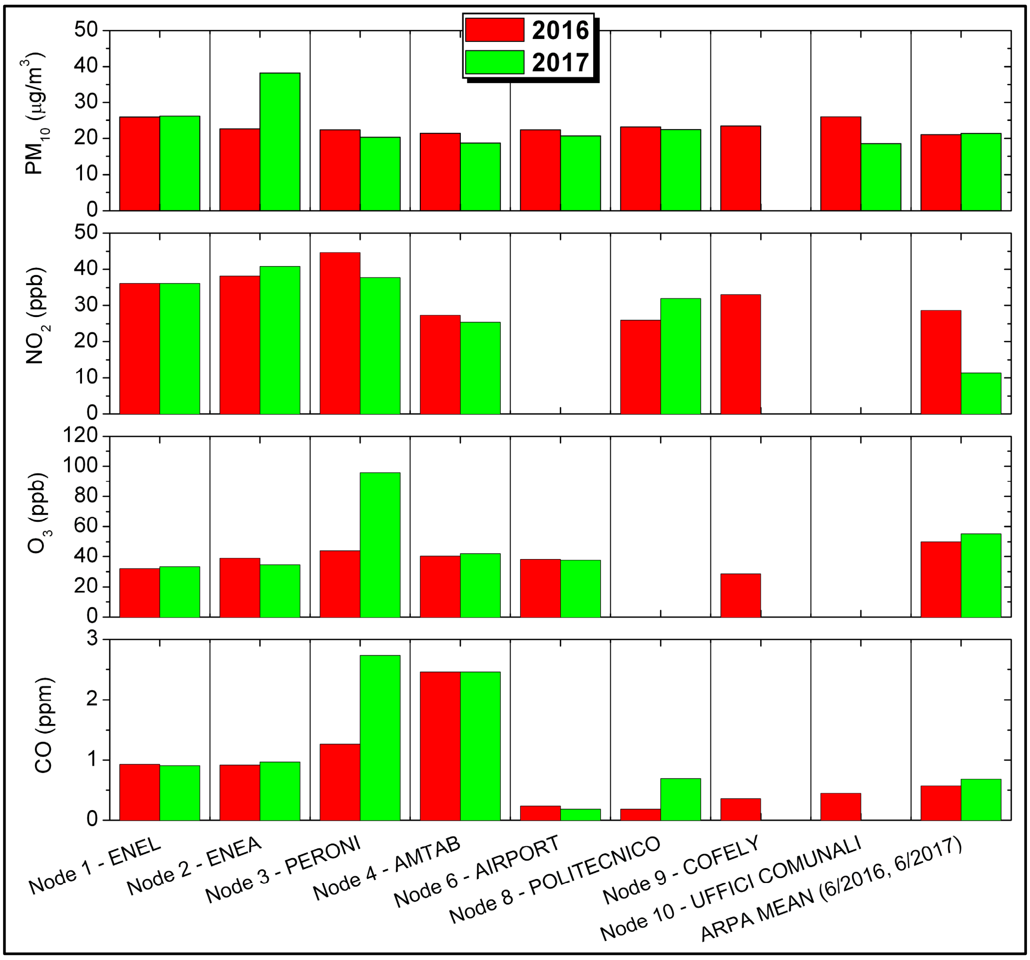

Figure 12. Comparison of the 2016 and 2017 yearly means of the sensor network (8 nodes) and related reference analyzer (Viale Kennedy: PM_{10}, NO_2, and O_3, and Via Cavour: CO) deployed in Bari city. The selected reference values for each pollutant are related to June 2016 and June 2017 as the annual mid-term. Some analyzer and sensor data are missing or not available.

For PM_{10} assessment, all nodes, excluding Node 2 in 2017, show a yearly mean comparable to the reference mean, exhibiting excellent accuracy in long-term operations. For NO_2 assessment, generally, the sensor nodes show values higher than reference analyzers with lower accuracy in real operations. For O_3 assessment, the sensor nodes, excluding Node 3 in 2017, show values comparable to reference analyzers with good accuracy in real operations. For CO assessment, some sensor nodes (Nodes 1, 2, 3, and 4) show values higher than reference analyzers with lower accuracy in real operations, and the remaining sensor nodes (Nodes 6, 8, 9, and 10) show values comparable to reference analyzers with better accuracy in real operations.

The performance discrepancy of the sensor nodes and reference analyzers could be attributed to local conditions of air pollution. In the next sections, a detailed analysis of each monitored air pollutant will be presented.

3.2.1. Particulate Matter (PM_{10})

Figure 13 shows the 2016 and 2017 trend of the monthly mean of the PM_{10} measured by eight sensor nodes (Shinyei, PPD20V) distributed in Bari city and compared to the monthly mean of the public reference data by air-quality monitoring stations operated by the local environmental agency. The monthly mean values do not exceed the limit of 50 μg/m^3, as regulated by EU Directive (2008/50/EC) in 2016 and 2017.

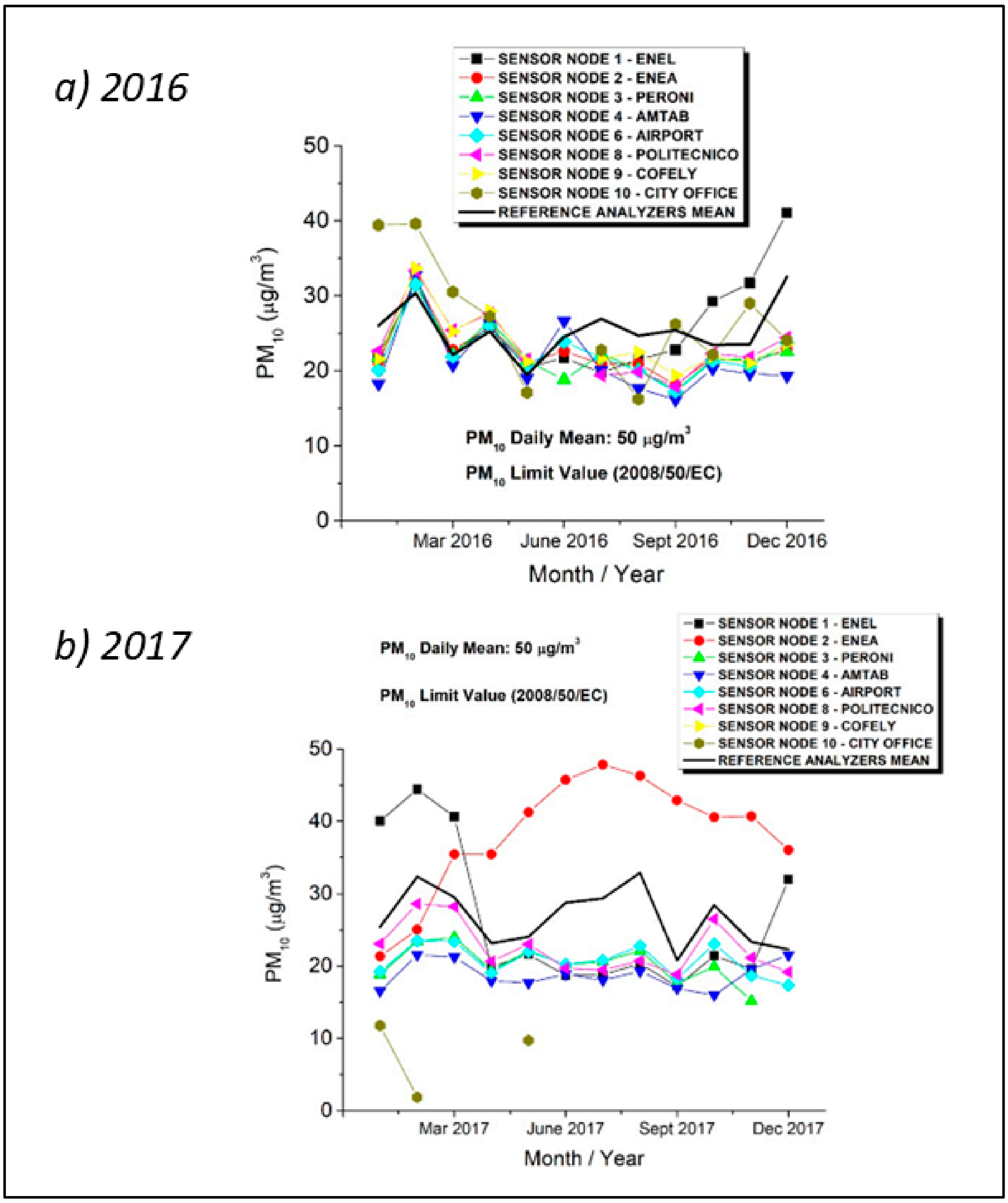

Figure 13. Trend of the PM_{10} monthly mean as measured by 8 urban sensor nodes (Shinyei, PPD20V) compared to the reference monthly mean measured by 8 air-quality monitoring stations of the ARPA-Puglia network in Bari city during (**a**) 2016 and (**b**) 2017.

However, in such cases, the daily mean values can exceed the regulated threshold, as shown in Figure 14. In fact, as an example, during February 2016 the comparison between sensor Node 2 (ENEA) and closest air quality station (Via Caldarola) reported exceedance over a threshold of 50 μg/m^3 in five specific days (15, 16, 17, 28, and 29 February) due to Saharan dust in Bari city, while the exceedance of 52 μg/m^3 that occurred on 24 February was due to an anthropogenic source: vehicular traffic. The high regression coefficient R of 0.84 and low Mean Absolute Error (MAE) of 8.1 μg/m^3 made the sensor node able to monitor the particulate matter in real time with good accuracy at the given location (ENEA office) for long-term operation.

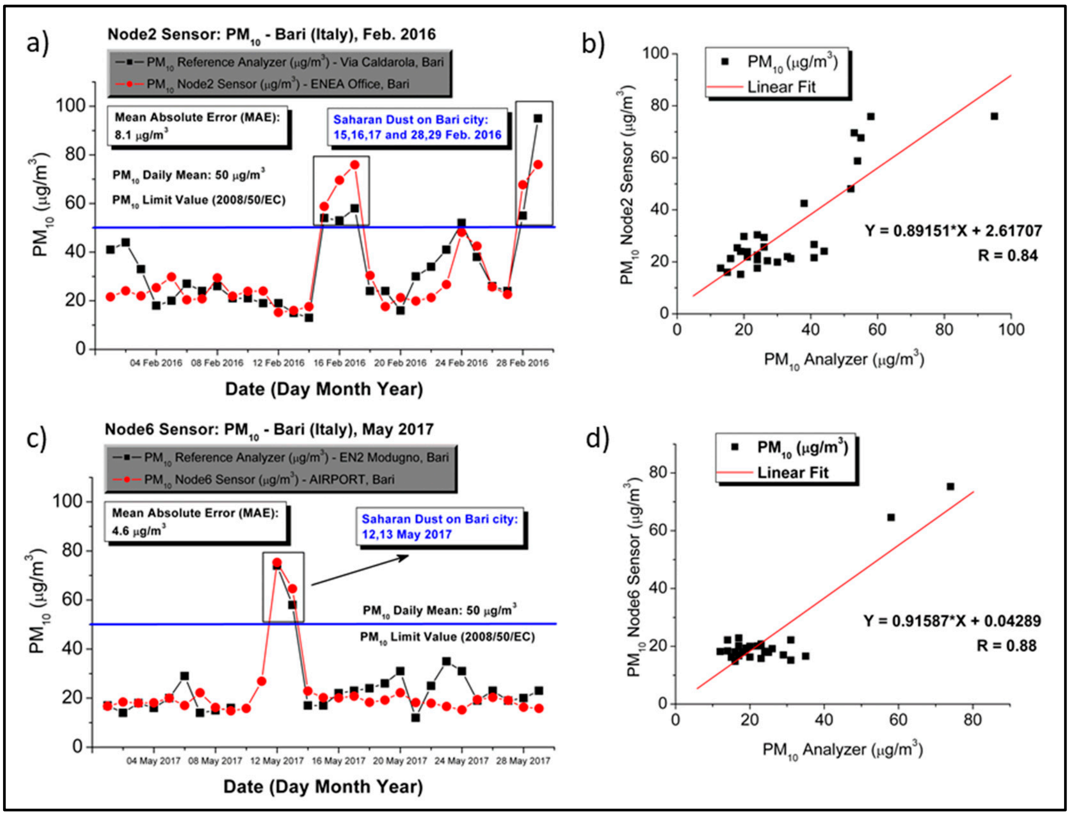

Figure 14. Sensor-versus-analyzer comparison of the daily mean to measure PM_{10} at (**a**) Node 2 (ENEA office) during February 2016 and related (**b**) regression coefficient (R), and at (**c**) Node 6 (Airport K. Wojtyla) during May 2017 and related (**d**) regression coefficient (R).

Additionally, during May 2017, the comparison between sensor Node 6 (Airport) and the closest air quality station (Modugno EN2) reported exceedance over a threshold of 50 μg/m^3 in two specific days (12 and 13 May) due to Saharan dust in Bari city, while no exceedance occurred due to anthropogenic sources. The high regression coefficient R of 0.88 and low Mean Absolute Error (MAE) of 4.6 μg/m^3 made the sensor node able to monitor the particulate matter in real time with good accuracy at the airport for long-term operations.

Table 3 reports on the performance of the sensor network, deployed in Bari city, for PM_{10} assessment during the years 2016 and 2017 using some specific indicators, such as yearly mean, Mean Absolute Error (MAE), relative error (RE), and regression coefficient (R) by comparison with the public official data of the closest air-quality monitoring station (AQMS), managed by the local environmental agency. The yearly means of each sensor node and closest AQMS are comparable with a MAE low value ranging from the lowest 2.49 μg/m^3 (COFELY) to the highest 8.16 μg/m^3 (AMTAB) in 2016, and from the lowest 5.10 μg/m^3 (POLITECNICO) to the highest 14.12 μg/m^3 (ENEA) in 2017. Usually, for each node, the MAE and RE tend to increase from 2016 to 2017 after continuous operations, indicating that the sensor performance becomes worse over time due to poisoning after 30 months of measurements. Finally, in 2016, the coefficient regression (R) shows high values (0.58–0.71) for five nodes (ENEL, ENEA, POLITECNICO, COFELY, and UFFICI COMUNALI) and low values (0.14–0.30) for three nodes (PERONI, AMTAB, and AIRPORT); while in 2017 R shows high values (0.48–0.76) for four nodes (PERONI, AIRPORT, POLITECNICO, and UFFICI COMUNALI) and low values (0.25–0.36) for three nodes (ENEL, ENEA, and AMTAB), with one node (COFELY) stopped in 2017 for an unavailable location. As a general rule, if R is lower than 0.5, then recalibration should be needed to enhance accuracy.

K.K. Johnson et al. [50] used the proposed PPD20V sensor to measure the fine particulate matter $PM_{2.5}$ at roadside sites in the cities of Atlanta (USA) and Hyderabad (India) to estimate the on-road emission factors by pairing $PM_{2.5}$, black carbon (BC), and carbon dioxide (CO_2) measurements.

Finally, in the present study, all PM_{10} sensor nodes, excluding Node 2 (ENEA) in 2017, exhibit a relative error of less than 50% (uncertainty of the EU Ambient Air Directive for Indicative Measurements) and, therefore, the Data Quality Objective (DQO) has been achieved by the sensor network during the 30-month operations (July 2015–December 2017).

3.2.2. Ozone (O_3)

Figure 15 shows the 2016 and 2017 trend of the monthly mean of the O_3 measured by 8 sensor nodes (Alphasense, O_3-B4) distributed in the Bari city and compared to the monthly mean of the public reference data by air-quality monitoring station (ARPA-Viale Kennedy) operated by the local environmental agency. The monthly mean values do not exceed the daily limit of 90 ppb (180 μg/m^3), as regulated by the EU Directive (2008/50/EC) in 2016 and 2017. As an example, during February 2017, the comparison between sensor Node 1 (ENEL) and the closest air quality station (Viale Kennedy) reported no exceedance over the threshold of 90 ppb (180 μg/m^3), as shown in Figure 16. Despite the low regression coefficient R of 0.23 (not shown), the combination of the low Mean Absolute Error (MAE) of 8.9 ppb and the relative error (RE) of 25.3% made the sensor node able to monitor the ozone in real time with an accuracy fitting the Indicative Measurements requirements at the given location (ENEL) for long-term operation.

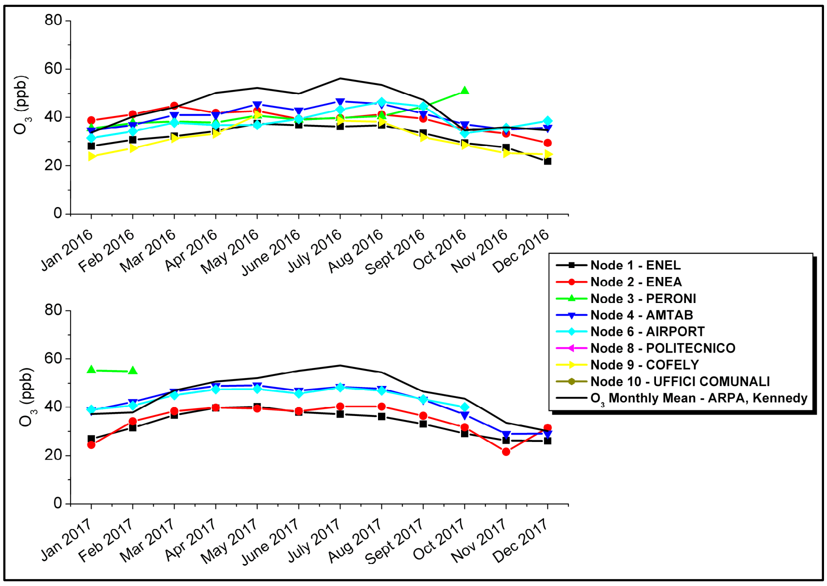

Figure 15. Trend of the O_3 monthly mean as measured by 8 sensor nodes (Alphasense, O_3-B4) compared to the reference monthly mean measured by a given air-quality monitoring station (Viale Kennedy, urban background) of the ARPA-Puglia network in Bari city in 2016 and 2017.

Table 3. Performance of the air quality sensor network (8 nodes) assessed by means of specific indicators related to PM10 in the years 2016 and 2017.

Node Info		**2016**					**2017**				
Node ID	**Node Location**	**Sensor Node PM_{10} Yearly Mean (μg/m^3)**	**Closest AQMS PM_{10} Yearly Mean (μg/m^3)**	**(*) Sensor Node PM_{10} Mean Absolute Error (μg/m^3)**	**(**) Sensor Node Relative Error (%)**	**Regression Coefficient (R)**	**Sensor Node PM_{10} Yearly Mean (μg/m^3)**	**Closest AQMS PM_{10} Yearly Mean (μg/m^3)**	**(*) Sensor Node PM_{10} Mean Absolute Error (μg/m^3)**	**(**) Sensor Node Relative Error (%)**	**Regression Coeffi-cient (R)**
Node 1	ENELVia Capruzzi	25.85	22.56	4.49	19.90	0.58	26.22	21.36	7.67	35.89	0.36
Node 2	ENEAViale Japigia	22.61	25.91	3.41	13.17	0.62	38.23	27.49	14.12	51.35	0.25
Node 3	PERONIVia Bitritto	22.32	26.67	7.78	29.16	0.30	20.31	29.85	10.30	34.52	0.76
Node 4	AMTABVia Jacobini	21.40	26.67	8.16	30.60	0.29	18.77	29.85	11.09	37.14	0.28
Node 6	AIRPORT WojtylaViale Ferrari	22.37	27.31	5.61	20.54	0.14	20.69	27.18	6.49	23.86	0.63
Node 8	POLITECNICOVia Amendola	23.14	25.91	3.29	12.68	0.67	22.42	27.49	5.10	18.55	0.48
Node 9	COFELYStrada Vassallo	23.39	24.98	2.49	9.97	0.71	n/a	27.16	n/a	n/a	n/a
Node 10	UFFICI COMU-NALIPiazza Ferrarese	25.94	24.69	4.85	19.63	0.65	33.47	26.34	7.78	29.52	0.62
	MEAN	**23.38**	**25.59**	**5.01**	**19.45**	**0.49**	**25.73**	**27.09**	**8.93**	**32.97**	**0.48**

(*) MAE = Mean Absolute Error. (**) Sensor Node Relative Error (SNRE) is defined as sensor MAE divided by AQMS Yearly Mean. (°) Sensor performance using the Min value instead of the Avg value for Node 10 only. In 2017, the node operated for only 3 months. (§) Node 9 was removed in December 2016. No data for 2017. n/a = not available.

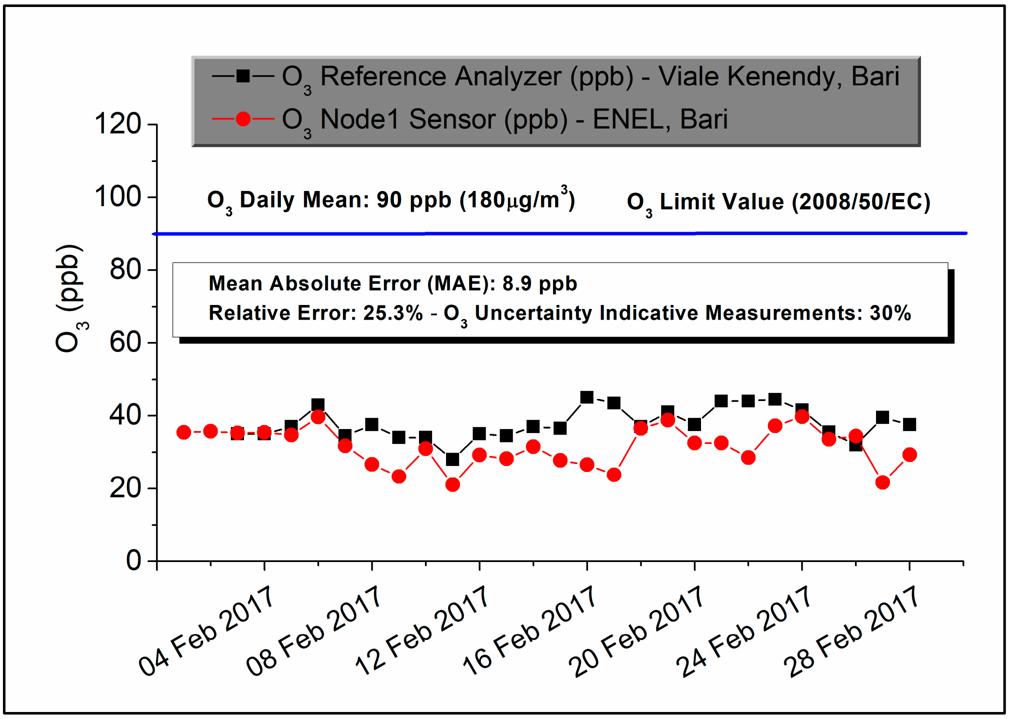

Figure 16. Sensor-versus-analyzer comparison of the daily mean to measure O_3 at Node 1 (ENEL) during Feb. 2017 and the related analyzer of the selected closest air-quality monitoring station (Viale Kennedy, urban background) of the ARPA-Puglia network in Bari city.

Table 4 reports on the performance of the sensor network, deployed in Bari city, for O_3 assessment during the years 2016 and 2017 using some specific indicators, such as yearly mean, Mean Absolute Error (MAE), relative error (RE), and regression coefficient (R) by comparison with the public official data of the closest air-quality monitoring station (ARPA-Viale Kennedy), classified as an urban background station and managed by local environmental agency. The ozone (O_3) is monitored by three air-quality monitoring stations only (Viale Kennedy Bari, CUS Bari, and EN2 Modugno) in Bari. The selection of the reference analyzer operated in Viale Kennedy has been made due to its having the best location in the centre of the city and its being symmetrically distant from all sensor nodes distributed in Bari. In fact, the other two air-quality monitoring stations (CUS Bari and EN2 Modugno) are asymmetrically located in the East and West urban peripheries. The yearly means of each sensor node and the selected AQMS are comparable with a MAE low value ranging from the lowest 4.88 ppb (AMTAB) to the highest 16.40 ppb (PERONI) in 2016, and from the lowest 3.80 ppb (AIRPORT) and 4.22 ppb (AMTAB) to the highest 17.64 ppb (PERONI) in 2017. Usually, for each node, the MAE and relative error (RE) tend to increase from 2016 to 2017 after continuous operations, indicating that the sensor performance became worse over time due to poisoning after 30 months of measurements. Finally, in 2016 the coefficient regression (R) shows high values (0.63–0.96) for five nodes (ENEL, ENEA, AMTAB, AIRPORT, and COFELY), and a low value (0.17) for one node (PERONI), and there were two nodes (POLITECNICO and UFFICI COMUNALI) with data not available; while in 2017 R shows high values (0.82–0.91) for four nodes (ENEL, ENEA, AMTAB, and AIRPORT), and a low value (0.10) for one node (PERONI), and there were three nodes (POLITECNICO, COFELY, and UFFICI COMUNALI) with data not available. As a general rule, if R is lower than 0.5, then recalibration should be needed to enhance accuracy. These R values, measured for ozone by this study, are comparable (R = 0.84) to the 18-day short-campaign (7–25 August 2015), using the same electrochemical O_3 sensor operated on the campus of the University of York (UK) [51].

Table 4. Performance of the air-quality sensor network (8 nodes) assessed by means of specific indicators related to O_3 in the years 2016 and 2017. The closest AQMS selected as a reference station is the ARPA-Viale Kennedy (urban background).

Node Info		**2016**					**2017**				
Node ID	**Node Location**	**Sensor Node O_3 Yearly Mean (μg/m^3)**	**Closest AQMS O_3 Yearly Mean (μg/m^3)**	**(*) Sensor Node O_3 Mean Absolute Error (μg/m^3)**	**(**) Sensor Node Relative Error (%)**	**Regression Coefficient (R)**	**Sensor Node O_3 Yearly Mean (μg/m^3)**	**Closest AQMS O_3 Yearly Mean (μg/m^3)**	**(*) Sensor Node O_3 Mean Absolute Error (μg/m^3)**	**(**) Sensor Node Relative Error (%)**	**Regression Coeffi-cient (R)**
Node 1	ENELVia Capruzzi	32.07	44.40	12.33	27.78	0.90	33.38	45.47	12.10	26.60	0.89
Node 2	ENEAViale Japigia	38.89	44.40	6.71	15.10	0.63	34.66	45.47	11.03	24.26	0.82
Node 3	PERONIVia Bitritto	44.16	44.40	16.40	36.93	0.17	55.10	45.47	17.64	38.80	0.10
Node 4	AMTABVia Jacobini	40.28	44.40	4.88	11.00	0.96	42.23	45.47	4.22	9.28	0.90
Node 6	AIRPORT WojtylaViale Ferrari	38.19	44.40	6.86	15.45	0.70	37.64	45.47	3.80	8.36	0.91
Node 8	POLITECNICOVia Amendola	n/a	44.40	n/a	n/a	n/a	n/a	45.47	n/a	n/a	n/a
Node 9	COFELYStrada Vassallo	28.66	44.40	11.58	26.08	0.93	n/a	45.47	n/a	n/a	n/a
Node 10	UFFICI COMUNALIPiazza Ferrarese	n/a	44.40	n/a	n/a	n/a	n/a	45.47	n/a	n/a	n/a
	MEAN	**37.04**	**44.40**	**9.79**	**22.05**	**0.71**	**40.60**	**45.47**	**9.75**	**21.46**	**0.72**

(*) MAE = Mean Absolute Error. (**) Sensor Node Relative Error (SNRE) is defined as sensor MAE divided by AQMS Yearly Mean. (°) Sensor performance using the Min value instead of the Avg value for Node 10 only. In 2017 nodes operated for 3 months only. (§) Node 9 was removed in December 2016. No data for 2017. n/a = not available.

Finally, in the present study, all O_3 sensor nodes, excluding Node 3 (PERONI) in 2016 and 2017, exhibit a relative error (RE) of less than 30% (uncertainty of the EU Ambient Air Directive for Indicative Measurements) and, therefore, the Data Quality Objective (DQO) has been achieved by the sensor network during the 30-month operations (July 2015–December 2017).

3.2.3. Nitrogen Dioxide (NO_2)

Figure 17 shows the 2016 and 2017 trend of the monthly mean of the NO_2 measured by eight sensor nodes (Alphasense, NO_2-B4) distributed in Bari city and compared to the monthly mean of the public reference data by the air-quality monitoring station (ARPA-Viale Kennedy) operated by the local environmental agency. The monthly mean values do not exceed the daily limit of 100 ppb (200 µg/m^3), as regulated by EU Directive (2008/50/EC) in 2016 and 2017. As an example, during February 2017, the comparison between sensor Node 1 (ENEL) and the closest air-quality station (Viale Kennedy) reported no exceedance over the threshold of 100 ppb (200 µg/m^3), as shown in Figure 18. The combination of the low regression coefficient R of 0.48 (not shown), the low Mean Absolute Error (MAE) of 11.8 ppb, and the relative error of 32% made the sensor node unable to monitor the nitrogen oxide in real time at the given location (ENEL) for long-term operation.

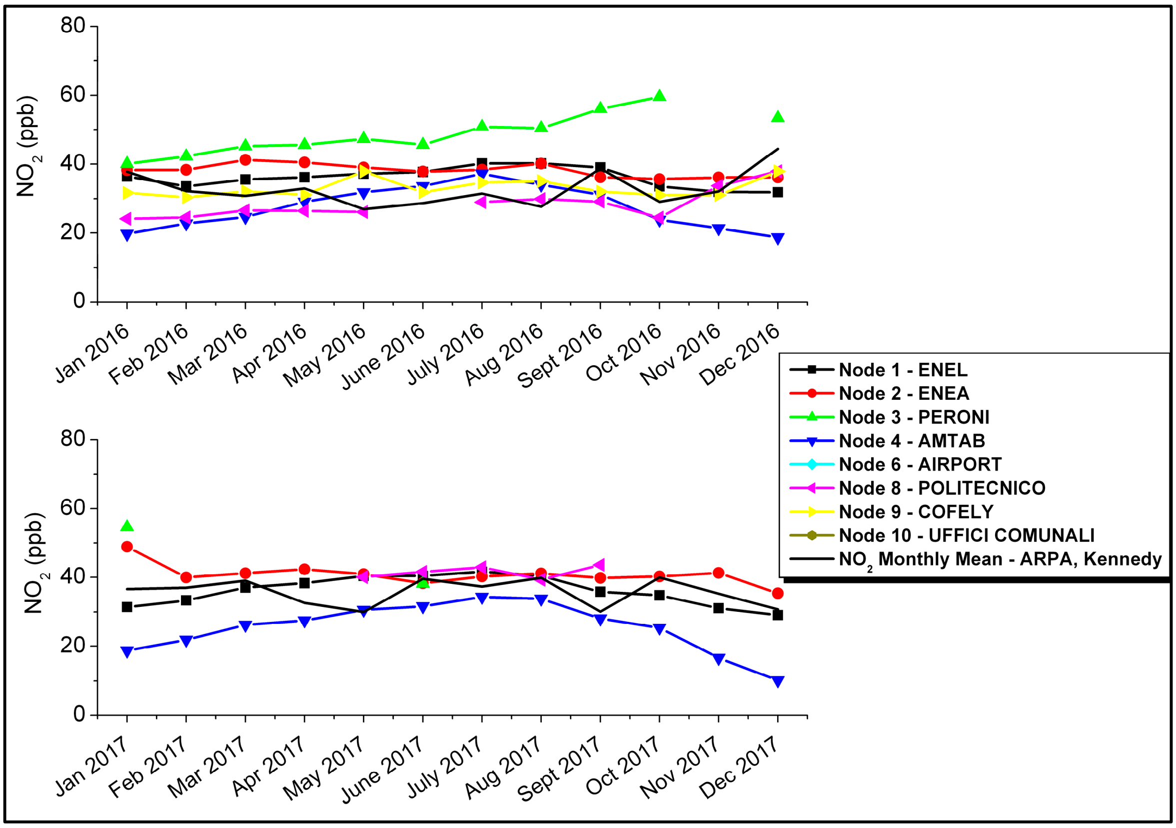

Figure 17. Trend of the NO_2 monthly mean as measured by 8 sensor nodes (Alphasense, NO_2-B4) compared to the reference monthly mean measured by a given air-quality monitoring station (Viale Kennedy, urban background) of the ARPA-Puglia network in Bari city in 2016 and 2017.

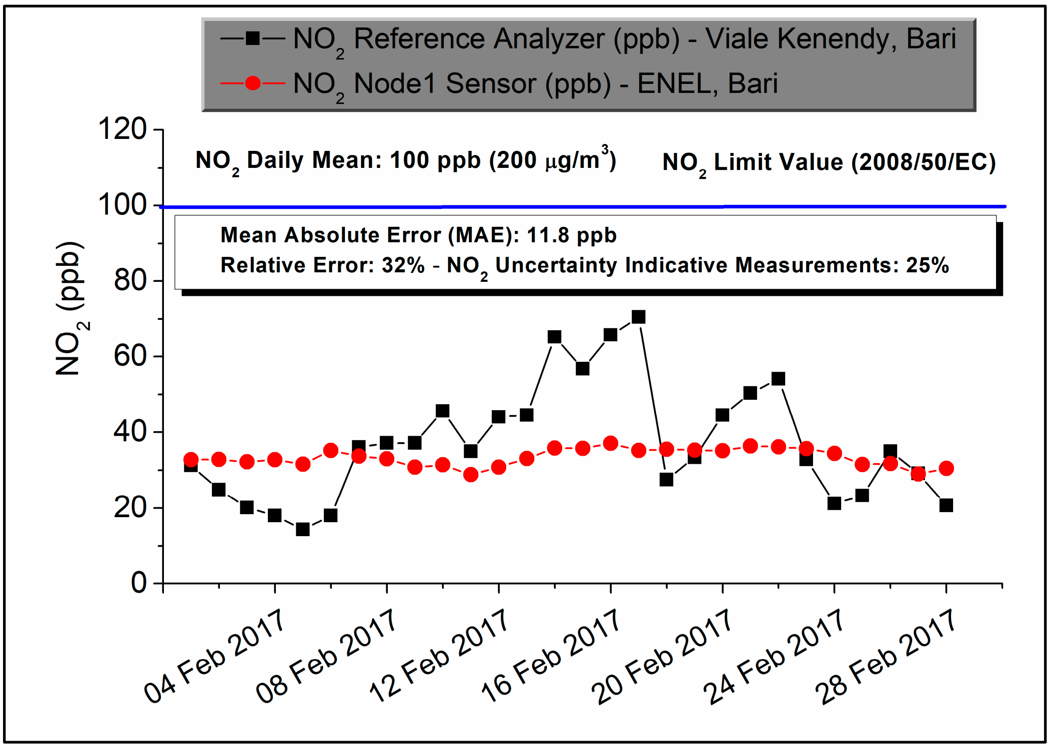

Figure 18. Sensor-versus-analyzer comparison of the daily mean to measure NO_2 at Node 1 (ENEL) during February 2017 and the related analyzer of the selected closest air-quality monitoring station (Viale Kennedy, urban background) of the ARPA-Puglia network in Bari city.

Table 5 reports on performance of the sensor network, deployed in the Bari city, for NO2 assessment during the years 2016 and 2017 using some specific indicators as yearly mean, Mean Absolute Error (MAE), relative error (RE) and regression coefficient (R) by comparison with the public official data of the closest air-quality monitoring station (ARPA-Viale Kennedy), classified as urban background station and managed by local environmental agency. The yearly means of each sensor node and the selected AQMS are comparable with a MAE low value ranging from the lowest 4.35 ppb (COFELY) to the highest 15.96 ppb (PERONI) in 2016, and from the lowest 4.10 ppb (ENEL) to the highest 18.03 ppb (POLITECNICO) in 2017. Usually, for each node the performance tends to decrease from 2016 to 2017 after continuous operations indicating poisoning after 30 months of measurements. Finally, in 2016 the coefficient regression (R) shows high values (0.41–0.53) for 3 nodes (ENEA, AMTAB, POLITECNICO), and a low value (0.10–0.33) for 3 nodes (ENEL, PERONI, COFELY), and 2 nodes (AIRPORT, UFFICI COMUNALI) with data not available; while in 2017 R shows low values (0.10–0.29) for 5 nodes (ENEL, ENEA, PERONI, AMTAB, POLITECNICO), and 3 nodes (AIRPORT, COFELY, UFFICI COMUNALI) with data not available. A periodical calibration should be carried out to enhance performance.

Finally, all NO_2 sensor nodes, excluding Node 3 (PERONI) in 2016 and 2017, Node 4 (AMTAB) in 2016 and 2017, and Node 8 (POLITECNICO) in 2017, exhibit relative error less than 25% (uncertainty of the EU Ambient Air Directive for Indicative Measurements) and, therefore, the Data Quality Objective (DQO) has been achieved by a few sensors of the network during 30-month operations (July 2015–December 2017).

Table 5. Performance of the air quality sensor network (8 nodes) assessed by means of specific indicators related to NO_2 in the year 2016 and 2017. The closest AQMS selected as reference station is the ARPA-Viale Kennedy (urban background).

Node Info		**2016**					**2017**				
Node ID	**Node Location**	**Sensor Node NO_2 Yearly Mean (µg/m^3)**	**Closest AQMS NO_2 Yearly Mean (µg/m^3)**	**(*) Sensor Node NO_2 Mean Absolute Error (µg/m^3)**	**(**) Sensor Node Relative Error (%)**	**Regression Coefficient (R)**	**Sensor Node NO_2 Yearly Mean (µg/m^3)**	**Closest AQMS NO_2 Yearly Mean (µg/m^3)**	**(*) Sensor Node NO_2 Mean Absolute Error (µg/m^3)**	**(**) Sensor Node Relative Error (%)**	**Regression Coeffi-cient (R)**
Node 1	ENELVia Capruzzi	36.13	32.74	5.72	17.48	0.33	36.13	35.67	4.10	11.51	0.22
Node 2	ENEAViale Japigia	38.16	32.74	7.21	22.04	0.41	40.78	35.67	5.32	14.93	0.16
Node 3	PERONIVia Bitritto	44.69	32.74	15.96	48.75	0.10	37.74	35.67	9.65	27.05	0.10
Node 4	AMTABVia Jacobini	27.33	32.74	9.08	27.74	0.53	25.41	35.67	10.36	29.05	0.29
Node 6	AIRPORT WojtylaViale Ferrari	n/a	32.74	n/a	n/a	n/a	n/a	35.67	n/a	n/a	n/a
Node 8	POLITECNICOVia Amendola	25.99	32.74	5.45	16.66	0.51	32.01	35.67	18.03	50.53	0.27
Node 9	COFELYStrada Vassallo	33.08	32.74	4.35	13.27	0.12	n/a	35.67	n/a	n/a	n/a
Node 10	UFFICI COMU-NALIPiazza Ferrarese	n/a	32.74	n/a	n/a	n/a	n/a	35.67	n/a	n/a	n/a
	MEAN	34.23	32.74	7.96	24.32	0.33	34.41	35.67	9.49	26.61	0.20

(*) MAE = Mean Absolute Error. (**) Sensor Node Relative Error (SNRE) is defined as sensor MAE divided by AQMS Yearly Mean. (°) Sensor performance using the Min value instead of the Avg value for Node 10 only. In 2017 node operated for 3 months only. (§) Node 9 was removed in December 2016. No data for 2017. n/a = not available.

Recently, a valid strategy to improve accuracy in the air quality sensors deployed in the real world is emerging as the field calibration by installing a reference instrument in the sensor network domain, as shown by the 50 nodes networked in the Berkeley Atmospheric CO_2 Observation Network (BEACO$_2$N) [30] for CO_2, CO, NO, NO_2, O_3 and PM_{10} monitoring; alternatively by the field stochastic calibration using dynamic neural network architectures demonstrated for NO_2, NO_x and O_3 [52].

3.2.4. Carbon Monoxide (CO)

Figure 19 shows the 2016 and 2017 trend of the monthly mean of the CO measured by 8 sensor nodes (Alphasense, CO-B4) distributed in the Bari city and compared to the monthly mean of the public reference data by air-quality monitoring station (ARPA-Via Cavour) operated by the local environmental agency. The monthly mean values do not exceed the daily limit of 8 ppm (10 mg/m^3), as regulated by EU Directive (2008/50/EC) in 2016 and 2017. As an example, during February 2017, the comparison between sensor node 1 (ENEL) and the closest air quality station (Via Cavour) reported no exceedance over the threshold of 8 ppm (10 mg/m^3), as shown in Figure 20. The combination of the medium regression coefficient R of 0.56 (not shown), the low Mean Absolute Error (MAE) of 0.23 ppm and the relative error of 17.3% made the sensor node able to monitor the level of the carbon monoxide in real time at the given location (ENEL) for long-term operation. However, a drawback of the CO sensor performance is the absence of seasonal variation as given by the ARPA instrument. In addition, the sensor ageing should be further investigated.

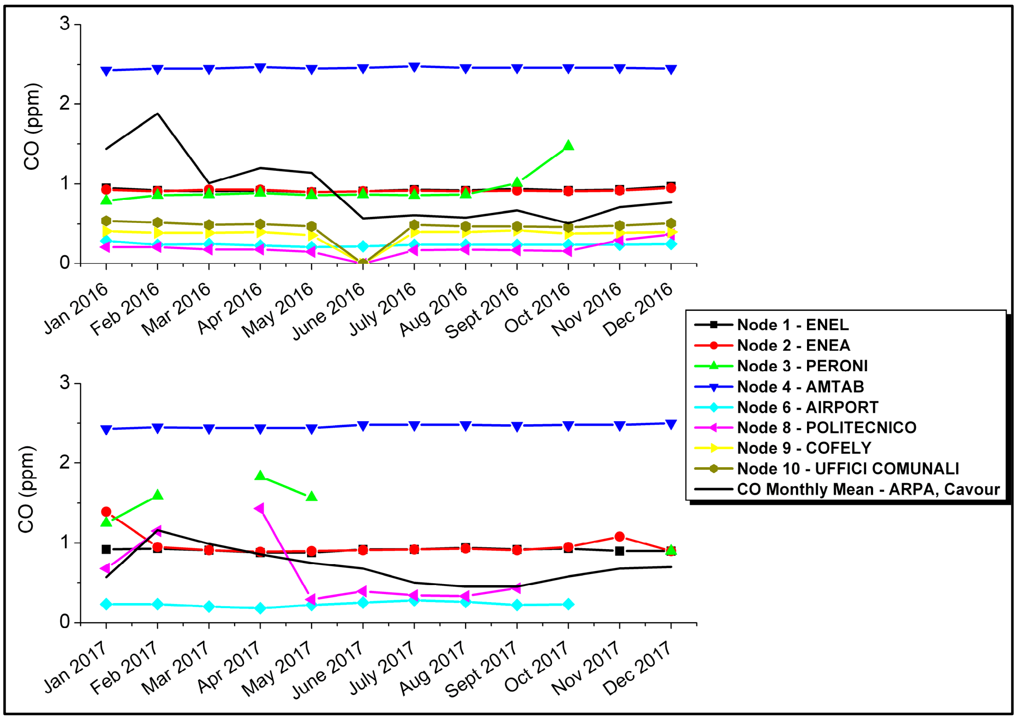

Figure 19. Trend of the CO monthly mean as measured by 8 sensor nodes (Alphasense, CO-B4) compared to the reference monthly mean measured by a given air-quality monitoring station (Via Cavour, urban traffic) of the ARPA-Puglia network in the Bari city on 2016 and 2017.

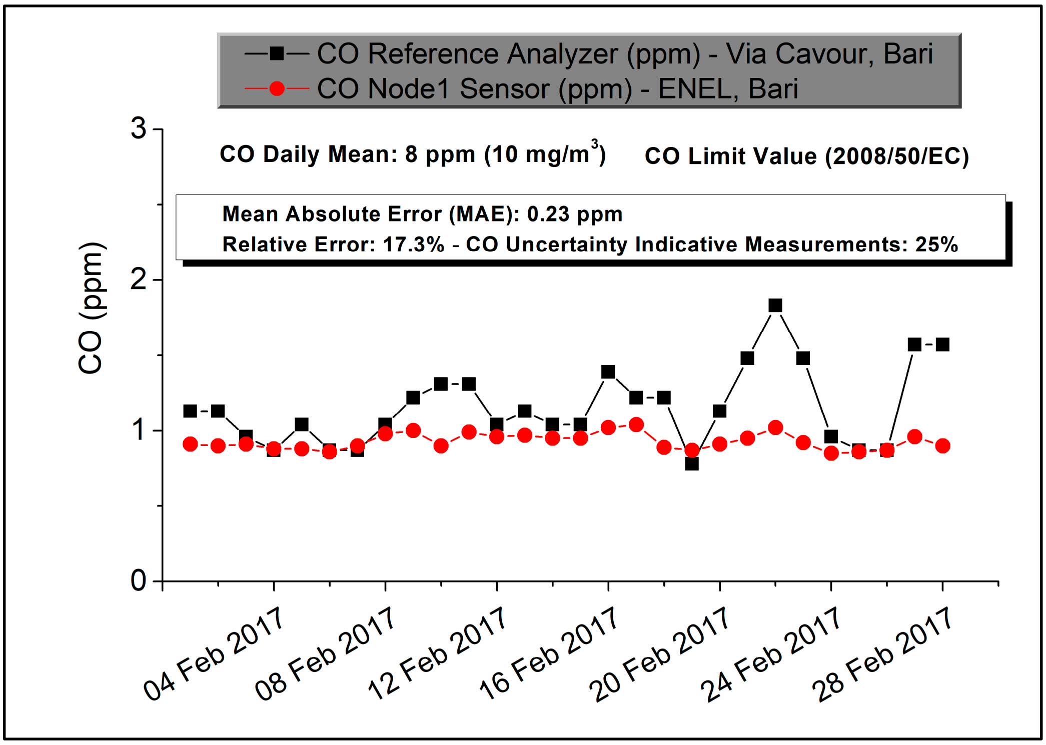

Figure 20. Sensor-versus-analyzer comparison of the daily mean to measure CO at Node 1 (ENEL) during February 2017 and related analyzer of the selected closest air-quality monitoring station (Via Cavour, urban traffic) of the ARPA-Puglia network in the Bari city.

Table 6 reports on performance of the sensor network, deployed in the Bari city, for CO assessment during the years 2016 and 2017 using some specific indicators as yearly mean, Mean Absolute Error (MAE), relative error (RE) and regression coefficient (R) by comparison with the public official data of the closest air-quality monitoring station (ARPA-Via Cavour), classified as an urban traffic station and managed by the local environmental agency. The yearly means of each sensor node and the selected AQMS are generally comparable, with a MAE low value ranging from the lowest 0.34 ppm (ENEA) to the highest 1.53 ppm (AMTAB) in 2016, and from the lowest 0.27 ppm (ENEL and POLITECNICO) to the highest 1.77 ppm (AMTAB) in 2017. Usually, for each node, the performance tends to degrade from 2016 to 2017 after continuous operations, indicating poisoning after 30 months of measurement. Finally, in 2016, the coefficient regression (R) shows values ranging from 0.10 to 0.72 for all nodes, with the highest value for node 10 (UFFICI COMUNALI); while in 2017, R shows values ranging from 0.18 to 0.52 for all nodes, with the highest value for Node 3 (PERONI) and Node 6 (AIRPORT), and two nodes (COFELY and UFFICI COMUNALI) with data not available. A periodical calibration should be carried out to enhance performance.

N. Masson et al. [53] studied a metal-oxide-based CO sensor, operated it for 19 days during April 2013 for air-quality monitoring, and installed it in downtown Denver (USA) adjacent to a busy motorway with significant CO pollution, and it reported a RMS error ranging from 0.22 to 0.48 ppm and a CO level ranging from 0.5 to 2.5 ppm. Temperature compensation techniques were used to reduce the sensor drift using a co-location reference analyzer by improving the correlation coefficient (R) up to 0.88.

Table 6. Performance of the air-quality sensor network (8 nodes) was assessed by means of specific indicators related to CO in the years 2016 and 2017. The closest AQMS selected as reference station is the ARPA-Via Cavour (urban traffic).

Node Info		2016					2017				
Node ID	**Node Location**	**Sensor Node CO Yearly Mean (μg/m^3)**	**Closest AQMS CO Yearly Mean (μg/m^3)**	**(*) Sensor Node CO Mean Absolute Error (μg/m^3)**	**(**) Sensor Node Relative Error (%)**	**Regression Coefficient (R)**	**Sensor Node CO Yearly Mean (μg/m^3)**	**Closest AQMS CO Yearly Mean (μg/m^3)**	**(*) Sensor Node CO Mean Absolute Error (μg/m^3)**	**(**) Sensor Node Relative Error (%)**	**Regression Coefficient (R)**
Node 1	ENELVia Capruzzi	0.93	0.92	0.35	37.47	0.10	0.91	0.70	0.27	38.10	0.27
Node 2	ENEAViale Japigia	0.92	0.92	0.34	36.75	0.02	0.97	0.70	0.32	45.81	0.18
Node 3	PERONIVia Bitritto	1.26	0.92	0.45	49.16	0.43	1.56	0.70	0.62	88.55	0.52
Node 4	AMTABVia Jacobini	2.46	0.92	1.53	165.95	0.52	2.46	0.70	1.77	252.86	0.46
Node 6	AIRPORT WojtylaViale Ferrari	0.24	0.92	0.68	74.12	0.25	0.19	0.70	0.51	72.45	0.52
Node 8	POLITECNICOVia Amendola	0.19	0.92	0.73	79.56	0.04	0.69	0.70	0.27	38.75	0.39
Node 9	COFELYStrada Vassallo	0.36	0.92	0.56	60.89	0.09	n/a	0.70	n/a	n/a	n/a
Node 10	UFFICI COMUNALIPiazza Ferrarese	0.45	0.92	0.47	51.40	0.72	n/a	0.70	n/a	n/a	n/a
	MEAN	**0.85**	**0.92**	**0.63**	**69.41**	**0.27**	**1.13**	**0.70**	**0.62**	**89.42**	**0.39**

(*) MAE = Mean Absolute Error. (**) Sensor Node Relative Error (SNRE) is defined as sensor MAE divided by AQMS Yearly Mean. (°) Sensor performance using the Min value instead of the Avg value for Node 10 only. In 2017, the node operated for 3 months only. (§) Node 9 was removed in December 2016. No data for 2017. n/a = not available.

Finally, in the present study, all CO sensor nodes exhibit a relative error (RE) higher than 25% (uncertainty of the EU Ambient Air Directive for Indicative Measurements) and, therefore, the Data Quality Objective (DQO) has not been achieved by any sensor of the network during the 30-month operations (July 2015–December 2017).

3.2.5. Carbon Dioxide (CO_2), Relative Humidity (RH), and Temperature (T)

Figure 21 shows the 2016 and 2017 trends of the monthly mean of carbon dioxide (CO_2), expressed in ppm, measured by the selected sensor (Alphasense, CO2-IRC-A1), of the urban relative humidity (RH), expressed in % unit, measured by the selected sensor (Honeywell, HIH5031), and of the urban temperature (T), expressed in Celsius degree (°C), measured by the selected sensor (Microchip, TC1047A), in the given Node 1 (ENEL) operated in the Bari city. The yearly mean values of CO_2 varied from 337 to 445 ppm with a yearly mean of 415 ppm in 2016, while the yearly mean values of CO_2 varied from 404 to 476 ppm with a yearly mean of 446 ppm in 2017. The high increase in the CO_2 concentration of 31 ppm between 2016 and 2017 could be attributed to the specific conditions of all the locations of the sensor nodes under test. However, the drift of the sensors could not be excluded and is worthy of further investigation. These data are affected by local micro-climate conditions but the annual trend is generally replicated during both years: in other terms, in the winter (D/J/F), the CO_2 is of a high value of about 480–490 ppm; in the spring (M/A/M), the CO_2 starts a decrease from about 460 to 380 ppm; in the summer (J/J/A), the CO_2 still continues a decrease from about 350 to 310 ppm; and, finally, in the autumn (S/O/N), the CO_2 starts a increase from about 390 to 460 ppm. The monthly lowest value of CO_2 in Node 1 is reached in July, as 312 ppm (2016) and 370 ppm (2017). The monthly highest value of CO_2 in Node 1 is reached in January 2016, at 494 ppm, and in December 2017, at 527 ppm.

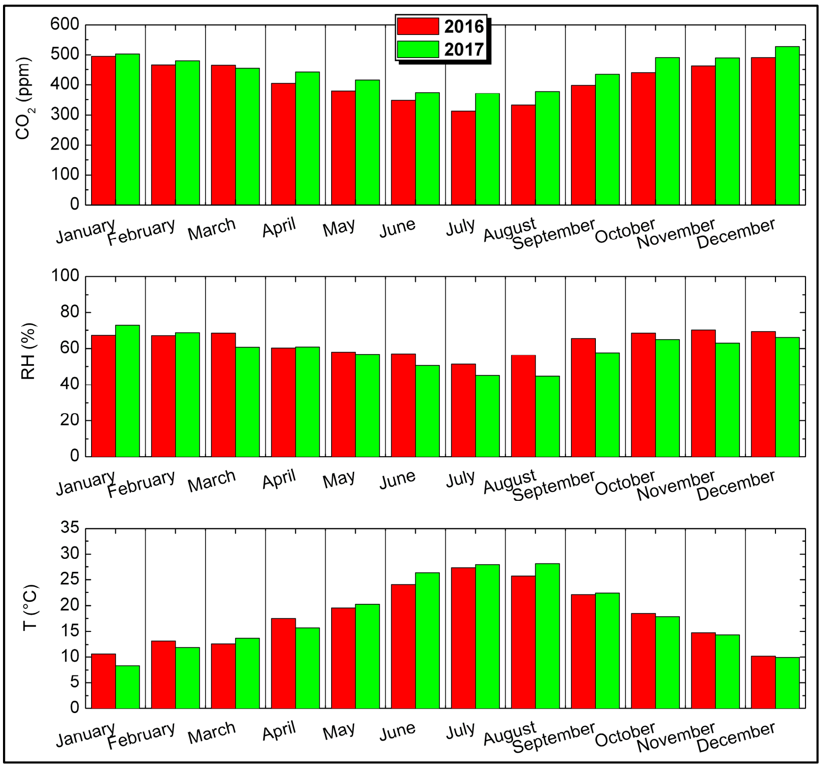

Figure 21. Trend of the carbon dioxide (CO_2), Relative Humidity (RH), and Temperature (T) monthly means as measured by a CO_2 sensor (Alphasense, CO_2-IRC-A1), a RH sensor (Honeywell, HIH5031), and a T sensor (Microchip, TC1047A), respectively, in the Node 1 (ENEL), deployed in Bari city during 2016 and 2017.

Furthermore, the yearly mean values of RH in Node 1 varied from 58.8% to 67.9% with a yearly mean of 63.2% in 2016, while the yearly mean values of RH varied from 55.0% to 63.9% with a yearly mean of 59.3% in 2017. The monthly lowest value of RH in Node 1 is reached in July 2016 as 51.3%, and in August 2017 as 44.8%.

The monthly highest value of RH in Node 1 is reached in November 2016 as 70.1%, and in January 2017 as 73.0%. Additionally, the yearly mean values of T in Node 1 varied from 17.2 °C to 18.8 °C, with a yearly mean of 18.0 °C in 2016, while the yearly mean values of T varied from 17.3 °C to 18.8 °C with a yearly mean of 18.0 °C in 2017.

The monthly lowest value of T in Node 1 is reached in December 2016 as 10.1 °C, and in January 2017 as 8.3 °C. The monthly highest value of T in Node 1 is reached in July 2016 as 27.3 °C, and in August 2017 as 28.0 °C. These data of the RH and T in Bari city (Southern Italy) are typical of a Mediterranean climate with a regular cycle of the seasons.

Sensor networks at low-cost and low power consumption have been used to monitor the urban CO_2 emissions in order to estimate the atmospheric inversion in the Paris area [54] using 70 sensor nodes; they are also used in California's Bay Area [55], using 34 sensor nodes of the Berkeley Atmospheric CO_2 Observation Network (BEACO2N), and covering an area of roughly 400 km^2; and, finally, they are used for urban CO_2 monitoring using 100 sensor nodes [56], operated in the Wuxi city, China. Since there was no common standard in the data format, a comparison cannot be proposed.

4. Discussion

The presented results of the long-term experimental campaign for urban air-quality monitoring in Bari city by a sensor network based on multiple nodes with multi-parametric sensors, such as particulate matter (PM_{10}), gases (NO_2, O_3, CO), and greenhouse gases (CO_2), and meteorological parameters, such as relative humidity (RH) and temperature (T), demonstrate the feasibility of the networked low-cost sensors in the framework of the Indicative Measurements of the EU Ambient Air Quality Directive. A comparison of the sensor performance has been realized using the official public data of the closest air-quality monitoring station (AQMS) of the urban network, operated and managed by the local environmental agency (ARPA-Puglia).

The assessment of the sensor-versus-analyzer inter-comparison has been carried out for PM_{10}, O_3, NO_2, and CO only, due to the availability of the reference public dataset. The results are reported in Figure 22. The figures of merit used for the assessment have been selected as the normalized error, defined as the sensor node relative error normalized to the Indicative Measurements, limits accuracy for each given pollutant, and the relative MAE, defined as the node yearly MAE normalized to the all-nodes mean MAE. If the normalized error is less than 1, then the data quality objective (DQO) for Indicative Measurements (see Section 1.3) has been achieved, while if the normalized error is higher than 1, then the sensor fails the regulatory issue of the data quality. Additionally, if the relative MAE is less than 1, the node sensor exhibits an error lower than the network mean, while if the relative MAE is higher than 1, the node sensor is at high error with poor precision.

By combining the normalized error and relative MAE, the best case for the sensor performance is with both parameters less than 1, and the worst case is with both parameters higher than 1; complementary cases to the best and worst cases are possible with medium performance. To show the long-term sensor assessment, four quadrants corresponding to the different combinations of normalized error with the relative MAE are shown in Figure 22. The performance assessment of the sensor network is summarized in Table 7.

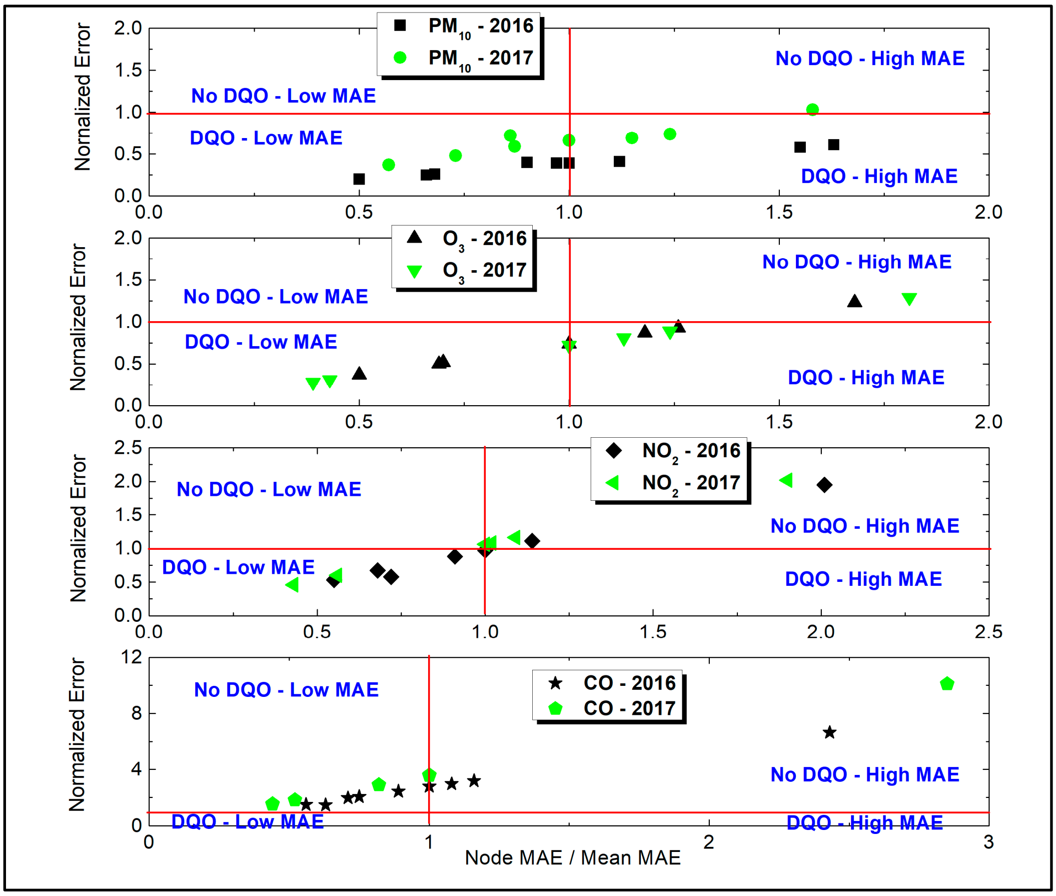

Figure 22. Assessment of the sensor performance for PM_{10}, O_3, NO_2, and CO related to the experimental campaign 2016 and 2017 in Bari city using Normalized Error (Sensor Node Relative Error/Indicative Measurements Limit Accuracy) versus Relative MAE (node MAE/mean MAE).

Table 7. Summary of the performance of the air quality sensor network deployed in Bari, assessed according to DQO as regulated by EU Directive (2008/50/EC). The figures of merit are defined in Appendix A.

Parameter	Normalized Error (NR)	Relative MAE (RMAE)	Performance Assessment of Sensor Network
PM_{10}	<1 (excluding Node 2 in 2017)	<1 (70% of Nodes)	Very Good
O_3	<1 (excluding Node 3 in 2016 and 2017)	<1 (50% of Nodes)	Good
NO_2	<1 (excluding Node 3 and Node 4 in 2016; and Node 3, Node 4, and Node 8 in 2017)	<1 (50% of Nodes)	Medium
CO	>1 (all Nodes)	<1 (70% of Nodes)	Poor

In terms of monthly average values, the PM_{10} sensor network exhibits a very good performance, fitting the Indicative Measurement requirements during 2016 and 2017 for all nodes, excluding Node 2 in 2017, with a normalized error less than 1, and a large part of the nodes with relative MAE less than 1. These results demonstrate that the sensor network has successfully reached the DQO for the Indicative Measurements in both years 2016 and 2017, with a low MAE in the majority of the nodes.

In terms of monthly average values, the O_3 sensor network exhibits good performance, fitting the Indicative Measurement requirements during 2016 and 2017 for all nodes, excluding Node 3 in 2016 and 2017, with a normalized error less than 1 and a 50% amount of the nodes with a relative MAE less than 1 only. These results demonstrate that the sensor network has successfully reached the DQO for the Indicative Measurements in both years 2016 and 2017, with a low MAE in half of the nodes.

In terms of monthly average values, the NO_2 sensor network exhibits a medium performance, fitting Indicative Measurement requirements during 2016 and 2017 for all nodes, excluding Node 3 and Node 4 in 2016, and the Node 3, Node 4, and Node 8 in 2017, with a normalized error of less than 1 and a 50% amount of the nodes with a relative MAE less than 1 only. These results demonstrate that the sensor network has successfully reached the DQO for the Indicative Measurements in both years 2016 and 2017, with a low MAE in the minority of the nodes.

In terms of monthly average values, the CO sensor network exhibits a poor performance, fitting Indicative Measurement requirements during 2016 and 2017 for all nodes, with no node at a normalized error less than 1, but 70% of the nodes had a relative MAE less than 1. These results demonstrate that the sensor network has not reached the DQO for the Indicative Measurements in both years 2016 and 2017. This low accuracy is caused by very low CO values measured in Bari city by the deployed sensors, increasing the error and worsening the performance.

Air sensors are useful to monitor the current status of atmospheric pollution at high spatial and temporal resolution for mapping urban and rural zones. Co-location of sensors and reference monitors is a valid approach to in-field calibration. So, the distance between sensors and reference analyzers should be as close as possible, if possible. However, air-quality monitoring stations are not located at high spatial resolution due to high cost. Thus, low-cost calibrated sensors are a good solution to monitor air quality, but they are affected by site specificity and local conditions. In our study, the PM sensors are very much able to detect high concentrations (>50 $\mu g/m^3$) of particulate matter, especially during the additional event of Saharan dust in Bari, which was measured by sensor Node 2 (ENEA) and referenced by the closest air-quality monitoring station (Via Caldarola), occurring on some days (15, 16, 17, 28, and 29) in February 2016; and this event was also measured by sensor Node 6 (Airport) and referenced by the closest air-quality monitoring station (Modugno EN2), occurring on some days (12 and 13) in May 2017. These PM sensors are at poor resolution in the range of low concentrations (10–40 $\mu g/m^3$), as reported in Figure 14; but they are very much able to differentiate high concentrations (> 50 $\mu g/m^3$), which is useful for the early detection of heavy dust in urban areas.

Generally, the performance of each sensor node depends strongly on the specific urban site that is affected by local ambient conditions in terms of temperature, humidity, and other interfering species. The ageing of the used air sensors is surely present in the long-term campaign in urban areas. Each designed sensor node has been deployed in a given urban site for the whole period of the experimental campaign. The exchange of a sensor node from one site to another is not the purpose of this work; the purpose is to check the best sensor performance in terms of ageing and the influence of location.

A comprehensive status of the urban air quality should include other biological pollutants not included in the European Ambient Air Directive (2008/50/EC), such as pesticides, pathogens, toxins, toxic elements, moulds, pollens, and other bio-chemicals. A review [57] of these topics is illustrated for environmental monitoring purposes.

Comprehensive reviews devoted to calibration, methods, and advanced technologies for wireless sensor networks deployed for air-quality monitoring have been proposed and studied in urban areas of all continents, including Europe [58], Australia [59], the USA [60], India [61], and a global overview [62].

5. Conclusions

In this paper, we demonstrate the feasibility of a sensor network based on 10 stationary nodes, distributed in Bari city (Southern Italy), in a city area of 24 km^2, for urban air-quality monitoring during a 30-month long-term campaign of continuous measurements. The stationary nodes have been installed outside in specific sites (e.g., the roof of buildings, offices, schools, streets, etc.) managed by partners and stakeholders of the Italian national project RES-NOVAE, under the supervision of the Bari energy manager. The location for each sensor-node AIRBOX, designed and developed by ENEA (Brindisi), has been selected, considering the closeness of a public air-quality monitoring station (AQMS) for reference validation. Continuous measurements have been realized for particulate matter (PM_{10}), gases (NO_2, O_3, CO), greenhouse gases (CO_2), and meteorological parameters such as relative humidity (RH) and temperature (T). A sensor-versus-analyzer inter-comparison has been realized in order to assess the sensor performance for selected air pollutants, such as particulate matter (PM_{10}) and gases (NO_2, O_3, CO). The selection of these four pollutants has been limited by official dataset availability as a reference.

In terms of monthly average values, the results show that PM_{10} sensor network exhibits a very good performance, fitting Indicative Measurement requirements during 2016 and 2017 for all nodes, excluding Node 2 in 2017, with low normalized error and low MAE in the large part of the nodes, successfully achieving the DQO for the Indicative Measurements in both years 2016 and 2017 in majority of the nodes.

In terms of monthly average values, the O_3 sensor network exhibits good performance, fitting Indicative Measurement requirements during 2016 and 2017 for all nodes, excluding Node 2 in 2017, with low normalized error and low MAE (50% of the nodes), successfully achieving the DQO for the Indicative Measurements in both years 2016 and 2017 in half of the nodes.

In terms of monthly average values, the NO_2 sensor network exhibits a medium performance, fitting Indicative Measurement requirements during 2016 and 2017, with low normalized error and low MAE (50% of the nodes), successfully achieving the DQO for the Indicative Measurements in both years 2016 and 2017 in the minority of the nodes.

In terms of monthly average values, the CO sensor network exhibits a poor performance fitting Indicative Measurement requirements during 2016 and 2017, with high normalized error and low MAE (70% of the nodes), failing the DQO for the Indicative Measurements in both years 2016 and 2017. This poor precision is ascribed to the low limit of the urban CO pollution, increasing the error in the measurement and decreasing the performance.

This study is one of a few cases to deploy a wireless sensor network, referenced by public official data, that operated for a 30-month long-term campaign of continuous monitoring, including a full pool of air pollutants using low-cost and low-power consumption sensors in an urban scenario.

Wireless sensor networks for air-quality monitoring are key to enabling technologies to develop the concept of the sustainable city [63] in the era of the Internet of Things (IoT), supporting decision-making and engaging citizens according to the goals of sustainable development.

Current research trends are exploring how to integrate low-cost air quality sensor networks with satellite monitoring systems to study ground-level pollution of main toxic gases and particulate matter at higher spatial and temporal resolutions [64,65].

Finally, our future work has been planned to monitor the chemical threat of fine particulate matter on human health, such as $PM_{2.5}$ and $PM_{1.0,}$ in urban areas.

Author Contributions: Conceptualization, M.P. (Michele Penza), D.S. and V.P.; methodology, M.P. (Michele Penza), M.P. (Mario Prato), S.D. and G.C.; software, D.S., M.P. (Mario Prato), V.P. and S.D.; validation, D.S., M.P. (Mario Prato), and S.D.; formal analysis, M.P. (Michele Penza); investigation, D.S., V.P., M.P. (Mario Prato), S.D. and G.C.; resources, M.P. (Michele Penza); data curation, V.P., M.P. (Mario Prato), and S.D.; writing—original draft preparation, M.P. (Michele Penza); writing—review and editing, M.P. (Michele Penza); visualization, S.D., V.P. and M.P. (Mario Prato); supervision, M.P. (Michele Penza); project administration, M.P. (Michele Penza); funding acquisition, M.P. (Michele Penza). All authors have read and agreed to the published version of the manuscript.

Funding: This work was financially supported by Italian project RES-NOVAE (PON04a2_E) *Networks, Buildings, Streets–New Challenging Targets for Environment and Energy* funded by the Italian Ministry of High Schools, University and Research (MIUR). Finally, the authors would like to acknowledge the support of the COST Action TD 1105–*European Network on New Sensing Technologies for Air-Pollution Control and Environmental Sustainability*—EuNetAir (2012–2016).

Data Availability Statement: The data presented in this study are available on request from the corresponding author due to some restrictions.

Acknowledgments: The authors wish to thank ARPA-Puglia for official air-quality public data, including partners and stakeholders such as IBM Italia, ENEL, ENEA (Bari), PERONI, AMTAB, POLITECNICO di Bari, COFELY, Aeroporti di Puglia, and the local authority of the Mayor of Bari, via City Energy Manager, for hosting a sensor-node and supporting the 30-month experimental campaign.

Conflicts of Interest: The authors declare no conflicts of interest.

Appendix A

Here, we define some figures of merit used in order to assess the sensor network performance:

- **Mean Absolute Error** (MAE) calculated as follows:

$$MAE = \frac{\sum_{i=1}^{n} |y_i - x_i|}{n} \tag{A1}$$

where y_i is the measured value by the sensor node for the ith observation, x_i is the measured value by the reference instrument for the ith observation, and n is the total number of observations. The lower the MAE is, the better the accuracy is.

- **Root Mean Square Error** (RMSE) calculated as follows:

$$RMSE = \sqrt{\frac{\sum_{i=1}^{n} \mid y_i - x_i \mid^{2}}{n}} \tag{A2}$$

where y_i is the measured value by the sensor node for the ith observation, x_i is the measured value by the reference instrument for the ith observation, and n is the total number of observations. The lower the RMSE is, the better the accuracy is.

- **Sensor Yearly Mean** (YM) calculated as follows:

$$SENS\ YM = \frac{\sum_{i=1}^{n} y_i}{n} \tag{A3}$$

where y_i is the measured value by the sensor node for the ith observation, and n is the total number of observations.

- **AQMS Yearly Mean** (AQMS YM) calculated as follows:

$$AQMS\ YM = \frac{\sum_{i=1}^{n} x_i}{n} \quad (A4)$$

where x_i is the measured value by an air quality monitoring station (AQMS) for the ith observation, and n is the total number of observations.

- **Sensor Node Relative Error** (SNRE) calculated as follows:

$$SNRE = \frac{Sensor\ MAE}{AQMS\ YM} \quad (A5)$$

where the indicators are defined in the equations above.

- **Normalized Error** (NE) calculated as follows:

$$NE = \frac{Sensor\ Node\ Relative\ Error\ (SNRE)}{Indicative\ Measurements\ Limit\ Accuracy\ (DQO)} \quad (A6)$$

where the indicators are defined in the equations above, and the *Indicative Measurements Limit Accuracy (DQO)* for each air pollutant is listed in Table A1 in Appendix B.

- **Relative MAE** (RMAE) calculated as follows:

$$RMAE = \frac{Sensor\ Node\ Yearly\ MAE}{All\ Nodes\ Mean\ MAE} \quad (A7)$$

where the indicators are defined above.

Appendix B

Here, we define some figures of merit used to assess the sensor performance:

- **Uncertainty—**The relative expanded uncertainty is estimated using Equation (A8), where x_i indicates the reference measurement, y_i the candidate method (sensor), and b_0 and b_1 are the slope and intercept of the orthogonal regression, respectively; RSS is the sum of squares of the residuals (Equation (A9)), and u is the uncertainty of the reference instrument. Further details on the calculation of the expanded uncertainty can be found in the *Guide for the demonstration of equivalence* [66] and Reports on Standards and Protocols of the Technical Committee *CEN/TC 264/WG 42/Ambient Air—Air quality sensors* [67]:

$$\mathrm{U_r}\ (\mathrm{y_i}) = \frac{2\left(\frac{RSS}{(n-2)} - u^2\ (x_i) + [b_0 + (b_1 - 1)x_i]^2\right)^{1/2}}{y_i} \quad (A8)$$

$$\mathrm{RSS} = \Sigma\ (\mathrm{y_i} - \mathrm{b_0} - \mathrm{b_1 x_i})^2 \quad (A9)$$

- Here, we report on uncertainty for *Fixed Measurement and Indicative Measurements as regulated by European Directive 2008/50/EC on Ambient Air Quality and Cleaner Air for Europe, art. 2.*

Table A1. Uncertainty of Fixed Measurements and Indicative Measurements by *European Directive 2008/50/EC on Ambient Air Quality and Cleaner Air for Europe, art. 2* [5].

Parameter	$NO_x/NO_2/NO$; CO; SO_2	C_6H_6	O_3	$PM_{10}/PM_{2.5}$
Uncertainty for *Fixed Measurements*	15%	25%	15%	25%
Uncertainty for *Indicative Measurements*	25%	30%	30%	50%

- Here, we report on uncertainty for *Fixed Measurement and Indicative Measurements as regulated by Directive of the European Parliament and of the Council on Ambient Air Quality and Cleaner Air for Europe dated 14 October 2024 (PE-CONS 88/24).*

Table A2. Uncertainty of Fixed Measurements and Indicative Measurements by *Directive of the European Parliament and of the Council on Ambient Air Quality and Cleaner Air for Europe dated on 14 October 2024 (PE-CONS 88/24)* [6].

Parameter	$NO_x/NO_2/NO$; CO; SO_2	C_6H_6	O_3	$PM_{10}/PM_{2.5}$
Uncertainty for *Fixed Measurements*	15%	25%	15%	25%
Uncertainty for *Indicative Measurements*	25%	35%	25%	50% (35%)

Indicative Measurements means measurements which meet Data Quality Objectives (DQO) that are less strict than those required for Fixed Measurements; *Fixed Measurements* means measurements taken at fixed sites to determine the levels in accordance with the relevant Data Quality Objectives (DQO). Fixed Measurements are mandatory in zones and agglomerations where the upper assessment thresholds are exceeded.

References

1. United Nations Environment Programme (UNEP). *Frontiers 2016 Report. Emerging Issues of Environmental Concern*; Job Nr: DEW/1973/NA; UNEP: Nairobi, Kenya, 2016; ISBN 978-92-807-3553-6. Available online: https://www.unep.org/resources/frontiers-2016-emerging-issues-environmental-concern (accessed on 10 April 2025).
2. European Environment Agency (EEA). *Air Quality in Europe—2017 Report*; EEA Report No. 13/2017; EEA: Copenhagen, Denmark, 2017; ISSN 1977-8449. Available online: https://www.eea.europa.eu/en/analysis/publications/air-quality-in-europe-2017 (accessed on 10 April 2025).
3. European Environment Agency (EEA). *Air Quality in Europe—2024 Report*; EEA Report No. ETC HE Report 2024/4; EEA: Copenhagen, Denmark, 2017; ISBN 978-82-93970-34-7. Available online: https://www.eionet.europa.eu/etcs/etc-he/products/etc-he-products/etc-he-reports/etc-he-report-2024-1-interim-air-quality-maps-of-eea-member-and-cooperating-countries-for-2023-pm-o3-and-no2-spatial-estimates-pm-o3-and-no2-spatial-estimates (accessed on 10 April 2025).
4. World Health Organization. Air Quality Guidelines for Particulate Matter, Ozone, Nitrogen Dioxide And Sulfur Dioxide. In *Global Update 2005. Summary of Risk Assessment*; WHO: Geneva, Switzerland, 2006; WHO/SDE/PHE/OEH/06.02; Available online: https://www.who.int/publications/i/item/WHO-SDE-PHE-OEH-06-02 (accessed on 10 April 2025).
5. Ambient Air Quality and Clean Air for Europe—EU Directive 2008/50/EC. Available online: http://eur-lex.europa.eu/legal-content/EN/TXT/PDF/?uri=CELEX:32008L0050&from=en (accessed on 10 April 2025).
6. Directive of the European Parliament and of the Council on Ambient Air Quality and Cleaner Air for Europe Dated on 14 October 2024 (PE-CONS 88/24). Available online: https://op.europa.eu/en/publication-detail/-/publication/efa5c00c-975b-11ef-a130-01aa75ed71a1/language-en (accessed on 25 October 2024).
7. Penza, M. Book Chapter Low-Cost Sensors for Outdoor Air Quality Monitoring. In *Advanced Nanomaterials for Inexpensive Gas Microsensors*; Llobet, E., Ed.; Elsevier: Amsterdam, The Netherlands, 2020; pp. 235–288. [CrossRef]
8. World Meteorological Organization. *An Update on Low-Cost Sensors for the Measurement of Atmospheric Composition*; 2021 WMO Report No. 1215; Peltier, R.E., Ed.; WMO: Geneva, Switzerland, 2021; ISBN 978-92-63-11215-6. Lead Authors: Castell, N., Clements, A.L., Dye, T., Hüglin, C., Kroll, J.H., Lung, S.-C.C., Ning, Z., Parsons, M., Penza, M., Reisen, F., von Schneidemesser, E. Available online: https://library.wmo.int/index.php?id=21508&lvl=notice_display#.Yifnz3yZPIU (accessed on 15 April 2025).
9. Williams, R.W.; Duvall, R.; Kilaru, V.; Hagler, G.; Hassinger, L.; Benedict, K.; Rice, J.; Kaufman, A.; Judge, R.; Pierce, G.; et al. Deliberating performance targets workshop: Potential paths for emerging $PM_{2.5}$ and O_3 air sensor. *Atmos. Environ. X* **2019**, *2*, 100031. [CrossRef]
10. Schneider, P.; Bartonova, A.; Castell, N.; Dauge, F.R.; Gerboles, M.; Hagler, G.S.W.; Hüglin, C.; Jones, R.L.; Khan, S.; Lewis, A.C.; et al. Toward a Unified Terminology of Processing Levels for Low-Cost Air-Quality Sensors. *Environ. Sci. Technol.* **2019**, *53*, 8485–8487. [CrossRef]
11. Dilonardo, E.; Palmisano, F.; Torsi, L.; Cioffi, N.; Penza, M.; Alvisi, M.; Di Franco, C. Evaluation of gas-sensing properties of ZnO nanostructures electrochemically doped with Au nanophases. *Beilstein J. Nanotechnol.* **2016**, *7*, 22–31. [CrossRef] [PubMed]
12. Penza, M.; Rossi, R.; Alvisi, M.; Serra, E.; Paolesse, R.; D'Amico, A.; Di Natale, C. Carbon nanotube films as a platform to transduce molecular recognition events in metalloporphyrins. *Nanotechnology* **2011**, *22*, 125502. [CrossRef] [PubMed]

13. Borrego, C.; Costa, A.M.; Ginja, J.; Amorim, M.; Coutinho, M.; Karatzas, K.; Sioumis, T.; Katsifarakis, N.; Konstantinidis, K.; De Vito, S.; et al. Assessment of air quality microsensors versus reference methods: The EuNetAir joint exercise. *Atmos. Environ.* **2016**, *147*, 246–263. [CrossRef]
14. Spinelle, L.; Gerboles, M.; Villani, M.G.; Aleixandre, M.; Bonavitacola, F. Field calibration of a cluster of low-cost available sensors for air quality monitoring. Part A: Ozone and nitrogen dioxide. *Sens. Actuators B Chem.* **2015**, *215*, 249–257. [CrossRef]
15. Spinelle, L.; Gerboles, M.; Villani, M.G.; Aleixandre, M.; Bonavitacola, F. Field calibration of a cluster of low-cost commercially available sensors for air quality monitoring. Part B: NO, CO and CO_2. *Sens. Actuators B Chem.* **2017**, *238*, 706–715. [CrossRef]
16. Castell, N.; Dauge, F.R.; Schneider, P.; Vogt, M.; Lerner, U.; Fishbain, B.; Broday, D.; Bartonova, A. Can commercial low-cost sensor platforms contribute to air quality monitoring and exposure estimates? *Environ. Int.* **2017**, *99*, 293–302. [CrossRef]
17. Jiao, W.; Hagler, G.; Williams, R.; Sharpe, R.; Brown, R.; Garver, D.; Judge, R.; Caudill, M.; Rickard, J.; Davis, M.; et al. Community Air Sensor Network (CAIRSENSE) project: Evaluation of low-cost sensor performance in a suburban environment in the southeastern United States. *Atmos. Meas. Tech.* **2016**, *9*, 5281–5292. [CrossRef]
18. Mead, M.I.; Popoola, O.A.M.; Stewart, G.B.; Landshoff, P.; Calleja, M.; Hayes, M.; Baldovi, J.J.; McLeod, M.W.; Hodgson, T.F.; Dicks, J.; et al. The use of electrochemical sensors for monitoring urban air quality in low-cost, high-density networks. *Atmos. Environ.* **2013**, *70*, 186–203. [CrossRef]
19. Baron, R.; Saffell, J.R. Amperometric gas sensors as a low-cost emerging technology platform for air quality monitoring applicThe Refations: A review. *ACS Sens.* **2017**, *2*, 1553–1566. [CrossRef]
20. North, R.J.; Cohen, J.; Wilkins, S.; Richards, M.; Hoose, N.; Polak, J.W.; Bell, M.C.; Blythe, P.T.; Sharif, B.; Neasham, J.; et al. Field deployment of the MESSAGE System for environmental monitoring. *Traffic Eng. Control* **2009**, *50*, 484–488.
21. Cohen, J.; North, R.J.; Wilkins, S.; Richards, M.; Hoose, N.; Polak, J.W.; Bell, M.C.; Blythe, P.T.; Sharif, B.; Neasham, J.; et al. Creating the MESSAGE Infrastructure. *Traffic Eng. Control* **2009**, *50*, 480–483.
22. Popoola, O.; Mead, I.; Bright, V.; Baron, R.; Saffell, J.; Stewart, G.; Kaye, P.; Jones, R. A Portable Low-Cost High Density Sensor Network for Air Quality at London Heathrow Airport. In Proceedings of the EGU General Assembly, Vienna, Austria, 7–12 April 2013; EGU: Munich, Germany, 2013. Available online: https://presentations.copernicus.org/EGU2013/EGU2013-1907_presentation.pdf (accessed on 11 April 2025).
23. Hasenfratz, D.; Saukh, O.; Walser, C.; Hueglin, C.; Fierz, M.; Arn, T.; Beutel, J.; Thiele, L. Deriving high-resolution urban air pollution maps using mobile sensor nodes. *Pervasive Mob. Comput.* **2015**, *16*, 268–285. [CrossRef]
24. Fishbain, B.; Lerner, U.; Castell, N.; Cole-Hunter, T.; Popoola, O.; Broday, D.M.; Martinez-Iniguez, T.; Nieuwenhuijsen, M.; Jovasevic-Stojanovic, M.; Topalovic, D.; et al. An evaluation tool kit of air quality micro-sensing units. *Sci. Total Environ.* **2017**, *575*, 639–648. [CrossRef] [PubMed]
25. The Copenhagen Wheel Project. Available online: https://senseable.mit.edu/copenhagenwheel/wheel.html (accessed on 17 January 2024).
26. Sun, L.; Wong, K.C.; Wei, P.; Ye, S.; Huang, H.; Yang, F.; Westerdahl, D.; Louie, P.K.K.; Luk, C.W.Y.; Ning, Z. Development and application of a next generation air sensor network for the Jong Kong marathon, 2015 air quality monitoring. *Sensors* **2016**, *16*, 211. [CrossRef]
27. Zhang, J.; Hu, J.; Huang, L.; Zhang, Z.; Ma, Y. A Portable Farmland Information Collection System with Multiple Sensors. *Sensors* **2016**, *16*, 1762. [CrossRef]
28. Choi, S.; Kim, N.; Cha, H.; Ha, R. Micro Sensor Node for Air Pollutant Monitoring: Hardware and Software Issues. *Sensors* **2009**, *9*, 7970–7987. [CrossRef]
29. Villa, T.F.; Salimi, F.; Morton, K.; Morawska, L.; Gonzalez, F. Development and Validation of a UAV Based System for Air Pollution Measurements. *Sensors* **2016**, *16*, 2202. [CrossRef]
30. Kim, J.; Shusterman, A.A.; Lieschke, K.J.; Newman, C.; Cohen, R.C. The Berkeley atmospheric CO_2 observation network: Field calibration and evaluation of low-cost air quality sensors. *Atmos. Meas. Tech. Discuss.* **2018**, *11*, 1937–1946. [CrossRef]
31. Cross, E.S.; Williams, L.R.; Lewis, D.K.; Magoon, G.R.; Onasch, T.B.; Kaminsky, M.L.; Worsnop, D.R.; Jayne, J.T. Use of electrochemical sensors for measurement of air pollution: Correcting interference response and validating measurements. *Atmos. Meas. Tech.* **2017**, *10*, 3575–3588. [CrossRef]
32. Heimann, I.; Bright, V.B.; McLeod, M.W.; Mead, M.I.; Popoola, O.A.M.; Stewart, G.B.; Jones, R.L. Source attribution of air pollution by spatial scale separation using high spatial density networks of low-cost air quality sensors. *Atmos. Environ.* **2015**, *113*, 10–19. [CrossRef]
33. van Zoest, V.; Osei, F.B.; Stein, A.; Hoek, G. Calibration of low-cost NO_2 sensors in an urban air quality network. *Atmos. Environ.* **2019**, *210*, 66–75. [CrossRef]
34. Kamińska, J.A.; Kazak, J.K. Indirect estimation of black carbon concentration in traffic site based on other pollutants—Time variability analysis. *J. Water Land Dev.* **2023**, *58*, 1–10. [CrossRef]
35. Yuval; Molho, H.M.; Zivan, O.; Broday, D.M.; Raz, R. Application of a sensor network of low-cost optical particle counters for assessing the impact of quarry emissions on its vicinity. *Atmos. Environ.* **2019**, *211*, 29–37. [CrossRef]

36. Hagan, D.H.; Isaacman-VanWertz, G.; Franklin, J.P.; Wallace, L.M.M.; Kocar, B.D.; Heald, C.L.; Kroll, J.H. Calibration and assessment of electrochemical air quality sensors by co-location with regulatory-grade instruments. *Atmos. Meas. Tech.* **2018**, *11*, 315–328. [CrossRef]
37. Feinberg, S.N.; Williams, R.; Hagler, G.; Low, J.; Smith, L.; Brown, R.; Garver, D.; Davis, M.; Morton, M.; Schaefer, J.; et al. Examining spatiotemporal variability of urban particulate matter and application of high-time resolution data from a network of low-cost air pollution sensors. *Atmos. Environ.* **2019**, *213*, 579–584. [CrossRef] [PubMed]
38. Kimbrough, S.; Krabbe, S.; Baldauf, R.; Barzyk, T.; Brown, M.; Brown, S.; Croghan, C.; Davis, M.; Deshmukh, P.; Duvall, R.; et al. The Kansas City Transportation and Local-Scale Air Quality Study (KC-TRAQS): Integration of Low-Cost Sensors and Reference Grade Monitoring in a Complex Metropolitan Area. Part 1: Overview of the Project. *Chemosensors* **2019**, *7*, 26. [CrossRef] [PubMed]
39. Miskell, G.; Alberti, K.; Feenstra, B.; Henshaw, G.S.; Papapostolou, V.; Patel, H.; Polidori, A.; Salmond, J.A.; Weissert, L.; Williams, D.E. Reliable data from low cost ozone sensors in a hierarchical network. *Atmos. Environ.* **2019**, *214*, 116870. [CrossRef]
40. Collier-Oxandale, A.; Feenstra, B.; Papapostolou, V.; Zhang, H.; Kuang, M.; Der Boghossian, B.; Polidori, A. Field and laboratory performance evaluations of 28 gas-phase air quality sensors by the AQ-SPEC program. *Atmos. Environ.* **2020**, *220*, 117092. [CrossRef]
41. da Silva Sousa, D.; Garcia Leal, V.; Trindade dos Reis, G.; Gonçalves da Silva, S.; Alves Cardoso, A.; da Silveira Petruci, J.F. An Automated, Self-Powered, and Integrated Analytical Platform for On-Line and In Situ Air Quality Monitoring. *Chemosensors* **2022**, *10*, 454. [CrossRef]
42. Wei, P.; Ning, Z.; Ye, S.; Sun, L.; Yang, F.; Wong, K.C.; Westerdahl, D.; Louie, P.K.K. Impact Analysis of Temperature and Humidity Conditions on Electrochemical Sensor Response in Ambient Air Quality Monitoring. *Sensors* **2018**, *18*, 59. [CrossRef]
43. Wang, W.-C.V.; Lung, S.-C.C.; Liu, C.-H. Application of Machine Learning for the in-Field Correction of a PM_2. *5 Low-Cost Sensor Network. Sensors* **2020**, *20*, 5002. [CrossRef]
44. Cao, R.; Li, B.; Wang, Z.; Peng, Z.-R.; Tao, S.; Lou, S. Using a distributed air sensor network to investigate the spatiotemporal patterns of $PM_{2.5}$ concentrations. *Environ. Pollut.* **2020**, *264*, 114549. [CrossRef]
45. Suriano, D.; Cassano, G.; Penza, M. Design and Development of a Flexible, Plug-and-Play, Cost-Effective Tool for on-Field Evaluation of Gas Sensors. *J. Sens.* **2020**, *2020*, 8812025. [CrossRef]
46. Penza, M.; Pfister, V.; Suriano, D.; Dipinto, S.; Prato, M.; Cassano, G. Application of low-cost sensors in stationary and mobile nodes for urban air quality index monitoring. *Eng. Proc.* **2023**, *48*, 62. [CrossRef]
47. Pfister, V.; Prato, M.; Penza, M. Field performance evaluation of air quality low-cost sensors deployed in a near-city space-airport. *Eng. Proc.* **2023**, *48*, 27. [CrossRef]
48. Müller, M.; Graf, P.; Meyer, J.; Pentina, A.; Brunner, D.; Perez-Cruz, F.; Hüglin, C.; Emmenegger, L. Integration and calibration of non-dispersive infrared (NDIR) CO_2 low-cost sensors and their operation in a sensor network covering Switzerland. *Atmos. Meas. Tech.* **2020**, *13*, 3815–3834. [CrossRef]
49. ARPA-Puglia—Local Environmental Protection Agency. 2025. Available online: https://dati.arpa.puglia.it/qaria (accessed on 17 January 2025).
50. Johnson, K.K.; Bergin, M.H.; Russell, A.G.; Hagler, G.S.W. Using low-cost sensors to measure ambient particulate matter concentrations and on-road emissions factors. *Atmos. Meas. Tech. Discuss.* **2016**, 1–22. [CrossRef]
51. Pang, X.; Shaw, M.D.; Lewis, A.C.; Carpenter, L.J.; Batchellier, T. Electrochemical ozone sensors: A miniaturised alternative for ozone measurements in laboratory experiments and air-quality monitoring. *Sens. Actuators B Chem.* **2017**, *240*, 829–837. [CrossRef]
52. Esposito, E.; De Vito, S.; Salvato, M.; Bright, V.; Jones, R.L.; Popoola, O. Dynamic neural network architectures for on field stochastic calibration of indicative low-cost air quality sensing systems. *Sens. Actuators B Chem.* **2016**, *231*, 701–713. [CrossRef]
53. Masson, N.; Piedrahita, R.; Hannigan, M. Approach for quantification of metal oxide type semiconductor gas sensors used for ambient air quality monitoring. *Sens. Actuators B Chem.* **2015**, *208*, 339–345. [CrossRef]
54. Wu, L.; Broquet, G.; Ciais, P.; Bellassen, V.; Vogel, F.; Chevallier, F.; Xueref-Remy, I.; Wang, Y. What would dense atmospheric observation networks bring to the quantification of city CO_2 emissions? *Atmos. Chem. Phys.* **2016**, *16*, 7743–7771. [CrossRef]
55. Turner, A.J.; Shusterman, A.A.; McDonald, B.C.; Teige, V.; Harley, R.A.; Cohen, R.C. Network design for quantifying urban CO_2 emissions: Assessing trade-offs between precision and network density. *Atmos. Chem. Phys.* **2016**, *16*, 13465–13475. [CrossRef]
56. Mao, X.; Miao, X.; He, Y.; Zhu, T.; Wang, J.; Dong, W.; Li, X.-Y.; Liu, Y. CitySee: Urban CO_2 measurements with sensors. In Proceedings of the IEEE Proceedings INFOCOM, Orlando, FL, USA, 25–30 March 2012; pp. 1611–1619. [CrossRef]
57. Justino, C.I.L.; Duarte, A.C.; Rocha-Santos, T.A.P. Recent progress in biosensors for environmental monitoring: A review. *Sensors* **2017**, *17*, 2918. [CrossRef]
58. Rai, A.C.; Kumar, P.; Pilla, F.; Skouloudis, A.N.; Di Sabatino, S.; Ratti, C.; Yasar, A.; Rickerby, D. End-user perspective of low-cost sensors for outdoor air pollution monitoring. *Sci. Total Environ.* **2017**, *607–608*, 691–705. [CrossRef]
59. Kang, Y.; Aye, L.; Ngo, T.D.; Zhou, J. Performance evaluation of low-cost air quality sensors: A review. *Sci. Total Environ.* **2022**, *818*, 151769. [CrossRef] [PubMed]

60. Liang, L. Calibrating low-cost sensors for ambient air monitoring: Techniques, trends, and challenges. *Environ. Res.* **2021**, *197*, 111163. [CrossRef]
61. Narayana, M.V.; Jalihal, D.; Nagendra, S.M.S. Establishing A Sustainable Low-Cost Air Quality Monitoring Setup: A Survey of the State-of-the-Art. *Sensors* **2022**, *22*, 394. [CrossRef]
62. Okorn, K.; Iraci, L.T. An overview of outdoor low-cost gas-phase air quality sensor deployments: Current efforts, trends, and limitations. *Atmos. Meas. Tech.* **2024**, *17*, 6425–6457. [CrossRef]
63. Kutami, M.; Takeno, M.; Ioka, H. New approach for environmental future city created by ICT: Sustainable city network. *FUJITSU Sci. Tech. J.* **2014**, *50–52*, 100–111.
64. Li, J.; Zhang, H.; Chao, C.-Y.; Chien, C.-H.; Wu, C.-Y.; Luo, C.H.; Chen, L.-J.; Biswas, P. Integrating low-cost air quality sensor networks with fixed and satellite monitoring systems to study ground-level $PM_{2.5}$. *Atmos. Environ.* **2020**, *223*, 117293. [CrossRef]
65. Rowley, A.; Karakuş, O. Predicting air quality via multimodal AI and satellite imagery. *Remote Sens. Environ.* **2023**, *293*, 113609. [CrossRef]
66. Guide for the Demonstration of Equivalence of Ambient Air Monitoring Methods. Available online: https://www.academia.edu/65705447/Guide_to_the_Demonstration_of_Equivalence_of_Ambient_Air_Monitoring_Methods (accessed on 30 April 2025).
67. Reports on Standards and Protocols of the Technical Committee CEN/TC 264/WG 42/Ambient Air—Air Quality Sensors. Available online: https://standards.iteh.ai/catalog/tc/cen/1dcd8f4d-521f-465f-af1c-91ef3e852bab/cen-tc-264-wg-42 (accessed on 30 April 2025).